FOLIO
TA7
C6
CER-58-2
cop 2

LIBRARIES
COLORADO STATE UNIVERSITY
FORT COLLINS, COLO.

FLUME STUDIES USING MEDIUM SAND (0.45 mm)

Geological Survey
Water-Supply Paper 1498-A

COLORADO STATE UNIVERSITY
LIBRARIES
JUL 14 1971

Simons, Richardson, and Albertson

CER58DBS2

Flume Studies Using Medium Sand (0.45 mm)

By D. B. SIMONS, E. V. RICHARDSON *and* M. L. ALBERTSON

STUDIES OF FLOW IN ALLUVIAL CHANNELS

GEOLOGICAL SURVEY WATER-SUPPLY PAPER 1498-A

A comprehensive study of fluvial hydraulics

UNITED STATES GOVERNMENT PRINTING OFFICE, WASHINGTON : 1961

UNITED STATES DEPARTMENT OF THE INTERIOR

STEWART L. UDALL, *Secretary*

GEOLOGICAL SURVEY

Thomas B. Nolan, *Director*

For sale by the Superintendent of Documents, U.S. Government Printing Office
Washington 25, D.C.

CONTENTS

ILLUSTRATIONS

TABLES

Symbols and Dimensions

		Dimensions	Units
A	Area of flow cross section	L^2	ft^2
B	Width of the flume	L	ft
$\frac{C}{\sqrt{g}}$	Chezy coefficient of discharge in dimensionless form which is equivalent to V/V_*.	O	
C_D	Drag coefficient for the particle	O	
C_T	Concentration of total load	ppm	
C_w	Concentration of fine material	ppm	
d	Median fall diameter of bed material	L	ft
d_t	Median fall diameter of total sediment load	L	ft
D	Average depth of flow	L	ft
Fr	Froude number $(V/\sqrt{gD})$	O	
g	Acceleration of gravity	L/T^2	ft/sec^2
G	Total load being transported	F/T	lbs/sec
h	Average height of bed roughness	L	ft
K	Any constant	O	
L	Average distance between features of bed roughness.	L	ft
n	Manning coefficient of roughness	$L^{1/6}$	$ft^{1/6}$
n_b	Manning coefficient of bed roughness (Einstein)	$L^{1/6}$	$ft^{1/6}$
P	Wetted perimeter	L	ft
Q	Discharge of water-sediment mixture	L^3/T	$ft^{3/sec}$
r	Relative coefficient of correlation	O	
R	Hydraulic radius (A/P)	L	ft
Re	Reynolds number VD/ν	O	
sf_c	Shape factor of the channel cross section	O	
sf_p	Shape factor of the sediment particle	O	
sf_r	Shape factor for the reach of the stream, sinuosity	O	
S	Slope of energy gradient equal to water surface slope in steady, uniform flow.	O	
t	Time	T	sec
T	Temperature	O	° C
V	Average velocity based on continuity principal	L/T	ft/sec
V_p	Average velocity based on velocity profiles	L/T	ft/sec
V_*	Shear velocity which is $\sqrt{gDS}$, $\sqrt{\tau_0/\rho}$	L/T	ft/sec
w	Fall velocity of sediment particles	L/T	ft/sec
γ	Specific weight of water	F/L^3	lbs/ft^3
γ_s	Specific weight of sediment	F/L^3	lbs/ft^3
$\Delta\gamma$	Difference between specific weights of air and water.	F/L^3	lbs/ft^3
$\Delta\gamma_s$	Difference between specific weights of sediment and water.	F/L^3	lbs/ft^3
δ'	Thickness of laminar sublayer	L	ft
ν	Kinematic viscosity	L^2/T	ft^2/sec
μ	Dynamic viscosity	Ft/L^2	$lb\text{-}sec/ft^2$

		Dimensions	Units
ρ	Density of water	Ft^2/L^4	$Slug/ft^3$
ρ_s	Density of sediment	Ft^2/L^4	$Slug/ft^3$
$\Delta\rho_s$	Difference between density of sediment and water.	Ft^2/L^4	$Slug/ft^3$
σ	Relative standard deviation of the size distribution of the sediment.	O	
τ_0	Tractive or shear force developed on the bed, γDS.	F/L^2	lbs/ft^2
τ_c	Critical tractive force associated with beginning of bed movement.	F/L^2	lbs/ft^2

GLOSSARY OF TERMS

Alluvial channel: A channel whose bed is composed of appreciable quantities of the sediments transported by the flow at a given discharge or greater.

Antidunes: Symmetrical sand and water-surface waves which are in phase, and which move upstream. The surface waves build up with time, becoming gradually steeper on their upstream sides until they break like surf and disappear. These waves usually develop, break, and reform in groups of two or more.

Bed material: The material of which a stream bed is composed.

Dune: A sand wave of approximately triangular cross section in a vertical plane in the direction of flow with gentle upstream slope and steep downstream slope. It travels downstream as a result of the movement of the sediment up the upstream slope and the deposition of part of this material on the downstream slope.

Equal transit rate (ETR): A method of sampling suspended sediment to obtain the mean concentration of the water-sediment mixture in the flume. By this method the depth integrating sampler (DH–48) is traversed through equally spaced verticals at an equal transit rate for each vertical.

Fall diameter: The diameter of a sphere that has a specific gravity of 2.65 and also has the same terminal uniform settling velocity as the particle (any specific gravity) when each is allowed to settle alone in quiescent distilled water of infinite extent and at a temperature of 24°C.

Median diameter: The midpoint in the size distribution of a sediment such that one-half of the weight of the material is composed of particles larger than the median diameter and the other one-half is composed of particles smaller than the median diameter.

Plane bed: A bed without elevations or depressions larger than the maximum size of the bed material.

Ripple: Small ridges and (or) crests, and troughs similar to dunes in shape, but smaller in magnitude, which have rather small width normal to the direction of flow.

Sand wave: A ridge (such as ripples, dunes, or symmetrical undulations) on the bed of an alluvial channel formed by the movement of the bed material.

Sediment: Fragmental material that originates from weathering of rocks and is transported by, suspended in, or deposited by water.

Sediment concentration: The ratio of dry weight of sediment to total weight of the water-sediment mixture, usually expressed in parts per million (ppm).

Standing waves: Symmetrical sand waves and water waves that are in phase and that gradually build up and just as gradually die down. Waves of this type are stationary, or essentially so, and usually develop in series and often reform, somewhat periodically, after disappearing.

Suspended load: The sediment moving in suspension in a fluid as a result of turbulent currents and (or) by colloidal suspension.

Total load: The total amount of sediment that is transported by water in a given length of time.

Fine material: That part of the total load composed of sizes not found in appreciable quantities in the bed material—normally the silt and clay sizes ($d<0.062$ mm).

STUDIES OF FLOW IN ALLUVIAL CHANNELS

FLUME STUDIES USING MEDIUM SAND (0.45 mm)

By D. B. SIMONS, E. V. RICHARDSON, and M. L. ALBERTSON

ABSTRACT

The results pertaining to the progress during the first year of a comprehensive study of fluvial hydraulics, specifically roughness in alluvial channels, are presented.

The report is based on the data collected by using a recirculating rectangular flume of adjustable slope, 8 feet wide, 2 feet deep, and 150 feet long with an alluvial bed of sand approximately 0.7 foot deep. A typical river sand has been utilized. Its median diameter, d, is 0.45 mm and its relative standard deviation, σ, is 1.60.

A total of 45 runs have been completed over a range of bed roughness forms extending from the plane bed with no movement to antidunes. In order to achieve this range, the discharge was varied from 2 to 21 cubic feet per second, the average velocity was varied from 0.5 to 7 feet per second, the average depth of flow was varied from 0.3 to 1.0 foot, and the slope of water surface was varied from 0.00014 to 0.01. Other variables measured included: water temperature, bed roughness, suspended sediment load, and total sediment load.

Terms describing channel roughness were formulated and tested based on the data collected. The results indicate, as one possibility, that the Chezy coefficient of discharge in dimensionless form $C/\sqrt{g}$ is a function of parameters involving the Froude number, viscosity of fluid, fall velocity, specific weight of the sediment, median diameter of the sediment particles and slope of the water surface. The various expressions presented were formulated on the fundamental concepts of fluid mechanics, dimensional analysis, and a detailed study of the variations of the variables measured.

In the two regimes of flow the following forms of bed roughness were observed.

For tranquil flow regime: plane bed without movement, ripples, dunes and transition from dunes to rapid flow forms.

For rapid flow regime: plane bed with movement, standing sand waves, and antidunes.

These forms of bed roughness are discussed and defined in various relationships.

Other data of both a laboratory and a field nature were combined with the flume data to develop a graphical relationship in which the form of bed roughness is related to size of bed material.

INTRODUCTION

The problem of defining roughness in alluvial channels dates back several centuries. A satisfactory solution of this problem has thus far eluded man. The principal reasons that only limited answers, which in some cases are of questionable value, have been developed are the

577668 O—61——2

broad scope of the problem and the multitude of variables influencing resistance to flow in alluvial channels. Alluvial channels are more complex than rigid channels because the form of the bed is a function of the flow and the bed material. That is, not only do the roughness elements resist the flow but they in turn are formed by the flow. In the experiments discussed in this report, the form of the bed was changed from plane to ripples, to dunes, and to antidunes by altering flow conditions. The resistance to the flow for each bed form is quite different. Thus far, most scientists working in this field have been limited by time, facilities, lack of instruments and fund. As a result only small parts of the complex problem have been thoroughly investigated. However, sufficient isolated groups of data have been collected and are being collected so that ultimately it should be possible to combine ideas and data resulting from these separate efforts to determine a general solution superior to any obtained thus far.

HISTORY

It is impossible to give proper credit to all who have made contributions of value in the field of fluvial hydraulics. Consequently, only a few of the more recent investigators whose work relates directly to resistance to flow in open channels will be cited.

One of the most thorough and complete groups of flume data ever collected resulted from a study by Gilbert (1914) which was sponsored by the U.S. Geological Survey and the University of California. He investigated the natural laws controlling the movement of material found on the beds of streams. The bed materials that he used consisted of sands and gravels obtained from typical California river beds. In all, more than one thousand tests were completed. These data have proved to be very valuable to the many investigators interested in flow in open channels.

Shields (1936) presented an analysis of the formation of roughness in stream beds. He proposed that the major parameters controlling bed undulations are $\tau_0/\Delta\rho d$ and $V_* d/\nu = 11.6\, d/\delta'$ in which

τ_0 = critical drag force per unit area
$\Delta\rho$ = submerged density of the particles
d = median diameter of the particles
δ' = thickness of the laminar sublayer
V_* = shear velocity
ν = kinematic viscosity

His parameters have been rather widely used in the analysis of problems involving drag and transportation of sediment.

The fundamental analyses that Einstein applied to sediment transportation (1950), to hydrodynamic forces on a rough wall

(Einstein and El-Sayed Ahamd El-Sammi, 1949), and to river channel roughness (Einstein and Barbarossa, 1951) have played an important role in stimulating interest and in providing a better understanding of the complexity of the laws of fluvial hydraulics and hydrodynamics.

Kalinske and Hsia (1945) presented the results of a study of the transportation of fine material by flowing water that is of importance because of the extremely small size of material used (d=0.011 mm). These data provide valuable information on how very fine material influences alluvial channel flow phenomenon.

The importance of fluvial morphology in the study of open channels was clearly defined by Lane (1955). An adequate understanding of this science is necessary to the understanding of stream forms and their behavior.

The hydraulic geometry of stream channels, as presented by Leopold and Maddock (1953), has contributed to a better understanding of the behavior of streams and rivers and verifies the existence of general laws that describe channel geometry. These laws are of the form developed for canals by Lindley, Lacey, Blench and others in India (Blench, 1957). That is, the wetted perimeter P, the hydraulic radius R, and the velocity V are all functions of the discharge Q.

Barton and Lin (1955) reported the results of a flume study done at Colorado State University, which was sponsored by the U.S. Army Corps of Engineers. The data presented therein were collected using a flume 80 feet long and 4 feet wide. The data, the collection procedures, and the analysis of the data are worthy of attention.

A study of roughness in alluvial channels by Ali and Albertson (1956) provides a qualitative expression defining roughness of the form

$$\frac{C}{\sqrt{g}}=\phi\left[Re, \frac{R}{d}\right]$$

and relating these variables to the transition function

$$\frac{C}{\sqrt{g}}-2\log\frac{R}{d}=\phi\left[\sqrt{32}\,\frac{Re}{\frac{R}{d}\,\frac{C}{\sqrt{g}}}\right]$$

C=Chezy coefficient
Re=Reynolds number
R=hydraulic radius
d=median diameter of bed material

Their work indicates that:

1. The laminar sublayer and Reynolds number are intimately related to the formation of ripples, dunes, and sand waves;

2. An increase in size of bed material decreases the influence of the laminar sublayer;
3. The normal sequence of the forms of bed roughness with increasing velocity is: no movement, ripples, dunes, sand waves, plane bed, and antidunes;
4. Other variables being held constant, the magnitude of bed roughness increases with a decrease in size of bed material within the noncohesive size range.

The effect of introducing fine material, clay size, on transportation of bed load was investigated in a turbulence tank by Makarechian.[1] He found that adding fines and holding the energy input constant does not dampen the turbulence appreciably, decreases the fall velocity of the sediment in transport; and increases the concentration at all points in the turbulent fluid.

Fine material may play an important role in channel stability, channel roughness, and sediment transport, since it causes an increase in viscosity and an increase in fluid density.

The analysis of sediment transportation by Bagnold (1956) is of importance to the study of roughness in alluvial channels, for, his concepts and equations provide a foundation from which predictions can be made regarding the influence of size and gradation of sediment on flow phenomenon. As the size of sediment is reduced, a size is reached where no additional energy input is required to transport additional quantities of this size and smaller. In fact, Bagnold's equations imply that the addition of very fine material may in effect impart energy to the flowing fluid. This concept is consistent with the results of the research in the turbulence tank done by Makarechian. It also compliments the current concepts proposed by many individuals working in the field of fluvial hydraulics concerning the influence of fine material on the behavior of fluvial streams.

A study of the theory of stable channels was completed by Simons and Albertson (1960). The field data presented therein should provide a valuable means of testing the results of laboratory studies of roughness in alluvial channels.

Liu (1957) presented a paper that explains accurately and in detail the mechanics of ripple formation. He concludes that ripples result primarily from the instability of the zone of large velocity gradient at the surface of the alluvial bed. He has formulated an experimental criterion that predicts the formation of ripples. That is,

---

[1] Makarechian, A. H., 1956, Effect of wash load on suspension of bed load: M.S. thesis, Colorado State University, Fort Collins, Colo.

the beginning of ripples is given by plotting experimental data in accordance with the functional relation.

$$\frac{V_*}{w}=\phi\left[\frac{V_* d}{\nu}\right]$$

where V_* = shear velocity
w = fall velocity
ν = kinematic viscosity
d = median diameter of bed material

The results of using these same parameters to define other regimes of bed roughness were presented by Albertson, Simons, and Richardson (1958).

Maddock (written communication, 1957) points out some of the significant factors of the foregoing analysis of ripple formation presented by Liu (1957) and also the importance of Durand's (1953) study on the transport of sediment in closed conduits. In addition, Maddock proposes that:

1. Sediment in motion should not be divided into a bed load and a wash load;
2. V_*, the shear velocity, is not a parameter of primary importance with respect to sediment movement;
3. Velocity distribution in alluvial channels is different from that in rigid boundary channels;
4. The shear velocity Reynolds number V_*D/ν is not directly related to sediment movement.

Finally, Maddock proposes a method for analysis of roughness in channel utilizing the concept that $C/\sqrt{g}$ probably consists of additive terms.

IMPORTANCE OF ROUGHNESS IN ALLUVIAL CHANNELS

The importance of accurately describing the resistance to flow or roughness in alluvial channels becomes immediately apparent when it is realized that the accurate evaluation of channel roughness is essential to the solution of all problems associated either directly or indirectly with water flowing on alluvial material. A more precise knowledge of channel roughness would assist materially in the design of stable channels. For example, slopes could be accurately determined consistent with existing conditions. Furthermore, an understanding of the behavior and control of rivers and river systems could be developed, and, the influence of imposing changes such as cutoffs, increasing or decreasing the sediment load, contractions at

bridges, and changing the characteristics of the sediment load could be predicted with greater precision.

In the design of hydraulic structures that are influenced by alluvial streams, or that influence the behavior of alluvial streams, an improved knowledge of channel roughness is a practical necessity. Here the applicability (or lack thereof) of data from the study of models to the prototype for flood routing, scour problems, backwater curve computations, and similar problems depends to a large extent on how accurately channel roughness can be estimated.

The accuracy with which discharge can be determined, excluding direct measurement, is a function of the accuracy with which channel roughness can be evaluated. Resistance to flow in alluvial channels varies between wide limits with discharge, temperature and size of bed material, and the magnitude and type of sediment load. As a result, a change in discharge may occur without a corresponding change in stage. The cost of flood control structures, bridges, and soil conservation methods is directly related to the accuracy with which floods can be measured.

These foregoing examples as well as many others, such as the influence of roughness on sediment transport, flow problems involving multiple roughness, all serve to illustrate the need for study and improvement of the knowledge of how and why channel roughness varies and how to evaluate its magnitude for any given set of conditions.

RESEARCH PROGRAM

In recognition of the need for a more basic and theoretical treatment of the science of fluvial hydraulics a research project was organized at Colorado State University in September 1956 to study the mechanics of water and sediment movement in alluvial channels. Since this is an extremely broad and complex field of study, it was decided to consider only one aspect of the total problem at a time, in order to minimize the diffusion of effort. The initial objective of this program, therefore, was the evaluation of bed roughness in alluvial channels, a subject of paramount importance, as already stated. This objective was further subdivided into a laboratory phase to be followed later by a field phase.

The project is a part of the research program of the Water Resources Division of the U.S. Geological Survey. P. C. Benedict and R. W. Carter assist with project planning and review of research developments. The study is under the supervision of S. K. Love, chief, Quality of Water Branch.

The laboratory studies of roughness in alluvial channels are being made in a recirculating laboratory flume 150 feet long, 8 feet wide and

2 feet deep with a sand bed. The flume is described in detail in the section, "Experimental equipment and procedure."

The investigation thus far done in the flume has involved:

1. Modification of the pumping system to meet the needs of the program;
2. Development of special techniques applicable to the measurement of the independent variables;
3. Selection and placement of a suitable sand to a depth of about 0.7 feet on the bed of the laboratory flume;
4. Collection of data for the sequence of runs thus far completed to obtain information on discharge, velocity, velocity distribution, slope, temperature, depth, bed roughness, total sediment load and photographs.

THEORY OF RESISTANCE TO FLOW IN ALLUVIAL CHANNELS

In a study of flow in alluvial channels, so many variables are involved that it is difficult to determine the fundamental relationship that exists between them. Fortunately, dimensional analysis can be employed so that the variables are arranged in dimensionless parameters to help reduce the number of variables, make the results applicable regardless of the system of units employed, and systematize the research and the analysis of data.

DEPENDENT AND INDEPENDENT VARIABLES

If the depth of flow D is selected as the single dependent variable for study, it will depend upon variables that fall into each of these four categories as follows:

$$D=\phi[\text{Geometry, flow, fluid, sediment}] \tag{1}$$

or more specifically

$$D=\phi_2[B, sf_c, sf_r, Q, S, \rho, \mu, \Delta\gamma, C_w, d, sf_p, \sigma, \Delta\gamma_s] \tag{2}$$

in which D is the only dependent variable and all the others are independent variables as defined in the list of symbols.

At this point it is important to be sure that each of the variables on the right side of equation 2 is actually independent and that each is necessary in determining the depth D. Frequently, in dimensional analysis, the mistake of inserting an extra dependent variable or extra independent variable is made. Such mistakes cause confusion that may be quite difficult to eliminate. Therefore, the initial selection of variables is worthy of considerable study before proceeding with the dimensional analysis.

The variables that describe the geometry of the channel are B, sf_c, and sf_r. The width of the channel B enters the problem because the discharge Q is distributed over this width, the width may control to some extent the secondary flow, and there may be one type of flow along one side of the channel and a different type of flow along the other side. If the shape of the cross section sf_c is varied, the depth of flow also varies to some extent. Although this variation may in some cases be relatively unimportant, the shape factor sf_c should, nonetheless, be included. The shape factor for the reach sf_r as measured by sinuosity may vary, affecting the depth, and should also be included. The flow variables are discharge Q and slope of the energy gradient S. The discharge Q is obviously of paramount importance because it can be varied at will, and such variation will cause the depth D also to vary. Since the slope can vary independently of the other variables and the depth of flow will then also vary, the slope S is both independent and of great importance. In establishing the depth of flow, no additional variables are needed to describe the geometry and the flow.

The variables that describe the fluid and influence the depth are the density ρ, the viscosity ν, and the difference in specific weight $\Delta\gamma$, across the interface of the lighter and heavier fluids at the surface. Density influences the depth because it expresses the mass effects and, therefore, is the heart of inertia, which plays a very important role in nearly all flow problems, aside from purely viscous flow (even here density seems to play an important part in describing completely the flow pattern, such as flow around tiny particles of sediment, for very small Reynolds numbers). Viscosity, quite obviously, has an influence because of its close association with boundary shear or drag and fall velocity.

The influence of $\Delta\gamma$ is not as obvious as that of viscosity. It is the fluid property that accounts for the influence of gravity. Actually, a stream is always submerged in an atmosphere of some kind. This atmosphere is usually air, but it might also be clear water with a stream of sediment-laden water (such as a density current in a reservoir) flowing under it, fresh water with a salt-water intrusion flowing under it, or warm water with a cold-water stream flowing under it. In each case it is the effective or submerged weight of the lower fluid that is important in reflecting the influence of gravity. If the atmosphere is air above water in an open channel, then $\Delta\gamma$ is essentially the same as the γ for the water. But if $\Delta\gamma$ is quite small, as for an interface of cold and warm fluids or for a salt water intrusion, then $\Delta\gamma$ must be considered as a factor. This is discussed in greater detail on page 9.

In brief, the fluid properties are very closely associated with motivating and retarding forces involved in open-channel flow. The effect of gravity, as reflected in $\Delta\gamma$ is to cause flow to take place; the viscosity is the important fluid property that resists flow causing shear; and inertia, as reflected in the density, ρ, is a property that resists any change in velocity (either in magnitude or direction). In steady, uniform flow the change in velocity is associated with turbulence and secondary circulation, which both play an important part in flow in open channels.

The properties of the sediment involved with flow in alluvial channels can best be described by the characteristic size d of the sediment in the bed, its characteristic size distribution as represented by σ, its characteristic shape factor sf_p, and the effective or submerged weight of the sediment.

The characteristic size d of the sediment is a subject of considerable discussion since it is intended that this size be the significant size. When there is a wide range of sizes, it is difficult to say whether the 50 percent size or some size smaller or larger is most significant. Until further information is available, the 50 percent size will be assumed as most representative and significant. The relative standard deviation is the second moment of the size distribution about the mean size, relative to the mean size. It may be dimensionless or not, depending upon the method of determination. The selection of the characteristic shape factor, like the diameter d, is subject to debate. In addition, it is difficult to measure shape of the particle. An indirect method would be to use Δd, the difference between the median diameter, as determined from mechanical analysis, and the median fall diameter, as determined by sedimentation methods, or to use a ratio of the two diameters. The ratio has the advantage that it would vary from 1 for perfect spheres, whereas the Δd would vary from 0 for perfect spheres. The shape factor may not be very important with ordinary sediments in the sand size range, as it may approach a constant. However, sf_p, d and $\Delta\gamma_s$ relate the interaction of the fluid and the sediment. Also d is involved as a grain roughness element, in addition to being related to the form of bed roughness, such as ripples and dunes. That is, with a plane bed condition the size of the sediment determines the roughness; with a dune bed condition the resistance to flow results from the bed configuration generated by the flow and d.

The use of $\Delta\gamma_s$ is another item that warrants discussion. Actually, $\Delta\gamma_s$ represents the effective specific weight of the particles of sediment, but it gives no clue whatsoever about either the density or the weight of a particle, except through gravitational acceleration, or the specific weight of the fluid. Basically, the question is which one is more

577668 O—61——3

important, the effective specific weight $\Delta\gamma_s$ of a particle or the actual density ρ_s of the particle. The $\Delta\gamma_s$ represents the net effect of gravity and hence the driving force causing downward motion, whereas ρ_s reflects the inertia of a particle that resists any change in velocity (either in magnitude or direction or both). The inertia may be of particular importance in the association of the particle with the turbulence of the flow and the consequent continual changing of velocity (both in magnitude and direction). But if a difference (such as $\Delta\gamma_s=\gamma_s-\gamma$ or $\Delta\rho_s=\rho_s-\rho$) is used instead of simply γ_s or ρ_s, then $\Delta\gamma_s$ is most significant.

The concentration of fine material C_w is a property of the fluid-sediment mixture, which actually changes the effective properties of the fluid. Past research, both in the laboratory and in the field, shows that as C_w is increased from small to large values, the concentration of the bed material load in suspension is increased. Therefore, C_w is of considerable importance.

THE PI-THEOREM

Using D, Q, and ρ as the repeating variables and applying the Pi-theorem to equation 2 yields

$$\phi_3\left[\frac{B}{D}, sf_c, sf_r, S, \frac{Q\rho}{\mu D}, \frac{Q^2}{\frac{\Delta\gamma}{\rho}D^5}, C_w, \frac{d}{D}, \frac{wD^2}{Q}, \sigma, \frac{Q^2}{\frac{\Delta\gamma_s}{\rho}D^5}\right]=0 \qquad (3)$$

In equation 2 the fall velocity w which relates the fluid and the sediment has been substituted for sf_p. The fall velocity depends on d, sf_p, $\Delta\gamma_s$ and μ, therefore it is not an independent variable. However, at this time it is the best measure of the interaction of the fluid and the sediment.

Although it is very helpful to use Q in determining equation 2, it is not usually included in the parameters involving μ, $\Delta\gamma$, w, and $\Delta\gamma_s$. If these parameters are multiplied by $(B/D)^n$ in such a way that Q is divided by the area BD, the velocity V can be substituted, which then makes these dimensionless parameters more significant. Equation 3 then becomes

$$\phi_4\left[\frac{B}{D}, sf_c, sf_r, S, \frac{VD\rho}{\mu}, \frac{V^2}{\frac{\Delta\gamma}{\rho}D}, C_w, \frac{d}{D}, \frac{w}{V}, \sigma, \frac{V^2}{\frac{\Delta\gamma_s}{\rho}D}\right]=0 \qquad (4)$$

The parameters involving μ and $\Delta\gamma$ can now be recognized as the Reynolds number and the Froude number, respectively. Furthermore, since $\Delta\gamma/\rho\approx g$ for flow of water in open channels, the Froude number can be put in the form

$$Fr=\frac{V}{\sqrt{gD}} \tag{5}$$

The last term in equation 4, and various other forms of it, have been much abused. Frequently, attempts have been made to call this term the Froude number of the particle when it is actually proportional to the drag coefficient, except that the depth D must be replaced by d, the velocity V must be replaced by the fall velocity w, and the inverse of the parameter must be used. Therefore, if the parameter is multiplied by D/d and $(w/V)^2$ and then taken to the minus-one power there results the drag coefficient C_D:

$$C_D \approx \frac{d\Delta\gamma_s}{\rho w^2}$$

which can be used to replace the last term in equation 4.

Equation 4 can now be written as

$$\phi_5\left[\frac{B}{D}, sf_c, sf_r, S, Re, Fr, C_w, \frac{d}{D}, \frac{w}{V}, \sigma, C_D\right]=0 \tag{6}$$

In some cases it is desired to involve viscosity in a Reynolds number of the falling particle Re_p instead of the Reynolds number of the flow Re_f. This can be done for equation 6 by multiplying the dimensionless Reynolds number term by w/V and d/D which yields

$$Re_p=\frac{VD}{\nu}\frac{w}{V}\frac{d}{D}=\frac{wd}{\nu} \tag{7}$$

and equation 6 can be rewritten as

$$\phi_6\left[\frac{B}{D}, sf_c, sf_r, S, Re_p, Fr, C_w, \frac{d}{D}, \frac{w}{V}, \sigma, C_D\right]=0 \tag{8}$$

Before equation 6 or 8 can be used satisfactorily, it is necessary to simplify them by reducing the number of terms being considered. This must be done with considerable care to be sure that important variables are not eliminated.

Laboratory investigations of alluvial channels and most field channels may be approximated by a rectangular shape. If this is not true in the field, it usually is due to one of the following three factors:

1. The channel is so wide, relative to the depth of flow and the size of the bed material, that two or more forms of bed roughness are existing side by side in the same channel. For example, there may be a deep part of the cross section and a shallow part, or a dune-covered part and a plane part or a combination

of these. Under these conditions the cross section should be divided into as many parts as necessary and usually each part can be approximated by a rectangular shape.

A potential danger in assuming that the channel can be separated into parts is the possibility of transverse flow between parts. Such flow has not been investigated but is probably of secondary importance.

2. The bed of part of the cross section may have rock or clay exposed so the channel is not truly alluvial throughout. By assuming, however, that the bed is completely alluvial and that all parts of the cross section can be represented by rectangular shapes, the shape factor term sf_c can be eliminated.
3. In the flume the sides of the channel are rigid and straight; consequently, the shape factor, sf_r can be eliminated.

The width-depth ratio B/D is a term that is probably of secondary importance provided $B/D \geq 5$. When $B/D < 5$, the resistance and other effects of the side walls or banks may become appreciable. The ratio may be of some importance for larger values, however, because of its relation to secondary flow and, possibly, its relation to three-dimensional flow. The actual phenomenon of secondary flow, as well as its importance, is not at all well understood. However, preliminary studies now under way indicate that a series of pairs of rotating vertical cells are formed under certain conditions. The extent to which the ratio B/D is associated with these cells, and the importance of the cells has not yet been established. However, the importance may be assumed for the present to be secondary compared with the other variables involved.

The concentration of the fine material C_w is a variable that enters the problem only if sediment is introduced that has a size smaller than that found in appreciable quantities in the bed material. If such material is introduced then C_w must be considered. Otherwise C_w may be neglected. The extent of the influence of this fine material has not yet been determined. On the one hand, sediment of a size appreciably smaller than those sizes found in appreciable quantities in the bed material will effectively increase the density and viscosity of the fluid. Consequently, research in the turbulence tank and data from the Colorado River have shown the concentration of bed-material load to be appreciably increased with fine material present over that concentration with clear water.

On the other hand, if the fine material introduced is just barely smaller than the bed material its influence is not known. It may increase the concentration of bed-material load, or it may decrease the concentration of the bed-material load if it acts to replace in part

the larger sizes. Fine material can be neglected only if there is none present.

The relative standard deviation σ of the size distribution of the bed material is a factor that is of considerable importance under certain conditions and, apparently, of much less or no importance under certain other conditions. In the unsteady process of scour, Thomas [2] has shown that the rate of sediment scour may be doubled by cutting the standard deviation in half. Liu (1957), however, has shown that ripples are initiated in sediments of the same median diameter, but of varying standard deviation, at about the same flow conditions. Since it is likely that ripple formation is more closely related to steady flow in alluvial channels than scour, the assumption can be made as a first approximation that the relative standard deviation σ is of secondary importance.

The use of the Froude number as a parameter has caused considerable controversy. Fundamentally, it expresses the ratio of the forces of inertia to the forces of gravity. It is important when the flow is accelerating either locally $\partial V/\partial t \neq 0$ or convectively $\partial V/\partial x \neq 0$. In other words, it can be important when the free surface flow involves unsteady flow or nonuniform flow. Unsteady flow exists when the velocity at a point is changing with time $\partial V/\partial t \neq 0$ as is reflected by increasing and decreasing discharge and velocity during a runoff event. Usually, if the rise and fall take place over a relatively long period of time the flow can be approximated as steady—that is $\partial V/\partial t \approx 0$. Nonuniform flow exists in most natural channels because of local expansion or contraction of the cross section. In uniform channels such as a laboratory flume or especially straight reaches of artificial channels, however, the flow can be assumed to be uniform. Nonuniformity in these cases may be due to backwater curves, surface waves or sand waves. It should be remembered that since velocity is a vector quantity, it has both direction and magnitude. Therefore, the flow is nonuniform if neither direction or magnitude changes with distance in the direction of flow.

Although there is little question that the Froude number enters the problem if surface waves are present, there is considerable controversy over the importance of the Froude number if sands waves are present on the bed without water waves at the surface. For example, as the flow passes over the crest of a dune, it is accelerated by the action of gravity, and the contact load of the sediment climbs the dune to the crest, beyond which it drops by gravitational action into the trough. Some scientists argue that gravitational action is inex-

[2] Thomas, R. K., 1953, Scour in a gravel bed: M.S. Thesis, Colorado State University, Fort Collins, Colo.

orably involved in this process and hence the Froude number is important. Conversely, other scientists argue that essentially the same accelerations of flow can take place in a closed conduit, owing to irregularities of the boundary where the driving force is due to a pressure gradient, rather than a sloping water surface or an energy gradient due to gravity. They further argue that in each case a gradient of piezometric head $P/\gamma+Z$ is the driving force, regardless of the cause. Finally, they point out that data taken from a closed conduit flowing full with an alluvial bed have given no conclusive evidence to prove that Froude number enters the problem. Also, Rouse (1950) states that with a completely confined flowing liquid gravitational acceleration does not effect the flow pattern, and, hence, there is no Froude number effect. When the Froude number has been used, in some cases it may be a modified coefficient of drag.

The Froude number Fr can be combined with the slope S to obtain the Chezy discharge coefficient $C/\sqrt{g}$. In so doing, either the slope or the Froude number apparently can be replaced by $C/\sqrt{g}$. Because the Froude number is so intimately related to the flow with water surface waves present, it is retained and the slope is dropped when $C/\sqrt{g}$ is included.

The need for some form of the Reynolds number to reflect the influence of viscosity has clearly been demonstrated by Ali and Albertson (1956), and by Liu (1957) to be important if the full significance of the phenomena associated with flow in alluvial channels is to be understood. Apparently, this can be accomplished by using the Reynolds number of the flow $Re_f=VD/\nu$ the Reynolds number of the particle $Re_p=wd/\nu$, or the shear velocity Reynolds number $Re_s=V_*d/\nu=11.6d/\delta'$, depending upon the particular need. The variable δ', is the thickness of the laminar sublayer.

The relative depth of flow D/d has been found to be important in rigid-boundary fluid mechanics as an expression of relative roughness. It is logical, therefore, that for certain conditions of flow in alluvial channels it would also be important. In addition to expressing the roughness of a plane bed relative to the depth of the flow, it also relates the size of the bed material to the scale of the flow system. Therefore, D/d is retained, at least for the present.

The relative fall velocity w/V is important in relating the fall velocity of the bed material to the velocity of the flow system. This parameter includes the influence of shape of the sediment particles and, together with the size ratio D/d and the drag coefficient C_D, may make it possible to compare the data taken with sediments of various specific weights in fluids of various specific weights.

In view of the foregoing discussions of the variables in equation 8, the following equations can be written

$$\phi_9[S, Re, Fr, D/d, w/V, C_D]=0 \tag{9}$$

or

$$\phi_{10}[C/\sqrt{g}, Re, Fr, D/d, w/V, C_D]=0 \tag{10}$$

Since

$$C/\sqrt{g}=\frac{V}{\sqrt{gDS}}=\frac{V}{\sqrt{\tau_0/\rho}}=\frac{V}{V_*} \tag{11}$$

equation 10 can be written as

$$\phi_{12}\left[\frac{V}{V_*}, Re, Fr, D/d, w/V, C_D\right]=0 \tag{12}$$

which now permits using $Re_*=\frac{V_*d}{\nu}$ and $\frac{V_*}{w}$ if so desired. Hence

$$\phi_{13}\left[\frac{V}{V_*}, Re_*, Fr, \frac{D}{d}, \frac{V_*}{w}, C_D\right]=0 \tag{13}$$

or

$$\phi_{14}\left[C/\sqrt{g}, Re, Fr, \frac{D}{d}, \frac{V_*}{w}, C_D\right]=0 \tag{14}$$

and

$$\phi_{15}\left[S, Re, Fr, \frac{D}{d}, \frac{V_*}{w}, C_D\right]=0 \tag{15}$$

in which Re can be any one of the three Reynolds numbers.

The drag coefficient C_D can be modified by combining it with V_*/w to yield $\tau_0/\Delta\gamma_s d$ which is a parameter frequently used, for example, by Shields and Einstein. This gives

$$\phi_{16}\left[S, Re, Fr, \frac{D}{d}, \frac{V_*}{w}, \frac{\tau_0}{\Delta\gamma_s d}\right]=0 \tag{16}$$

Various combinations of these variables can be used to satisfy the particular problem in question. All are equally valid theoretically but certain ones may produce better and more significant relationships than others.

The foregoing equations may satisfactorily introduce all of the dimensionless parameters necessary to analyze correctly the problem of resistance to flow in alluvial channels. On the other hand it may be that even more significant groups of parameters can be established That is, it may be desirable to evaluate all possible Pi-terms and then select $n-k$ of them for the final relationship in which n is the total number of variables, and k is the number of physical dimensions, 3 in this case. All of the possible Pi-terms can be evaluated by the

same procedure used to introduce the Reynolds number for the particle Re_p and the coefficient of drag for the particle C_D or, as another possibility, various repeating variables can be selected and Pi-terms evaluated until all terms have been used as repeating variables. This procedure yields all possible terms in their most simple form.

The total number N of possible Pi-terms can be determined, according to Van Driest (1946), by the equation

$$N=\frac{n!}{(k+1)\,!(N-k-1)\,!}$$

where n and k are defined as in the foregoing paragraph. To illustrate (three physical dimensions being involved, $k=3$) 5 variables yield 5 possible Pi-terms, 6 variables yield 15 possible Pi-terms and 7 variables yield 35 possible Pi-terms, however, not more than $n-k$ of these Pi-terms should be included in any one functional relationship.

As a final possibility, not introduced thus far, there also exists the possibility of adding still more dimensionless Pi-terms by considering new terms formulated by taking sums and (or) differences of existing terms. Such an approach could be justified if indicated by a mathematical model or even by simple logical reasoning.

Other parameters of interest, some dimensional and others nondimensional (the latter group being formulated as indicated in the foregoing paragraphs), that will be utilized in the analysis of data as follows:

C_T is the concentration of total load in ppm.

G is the total sediment load.

$\frac{C}{\sqrt{g}}$ is the Chezy discharge coefficient in dimensionless form.

n is the Manning coefficient of roughness.

τ_0 is the shear or tractive force exerted on the bed by the flowing mixture of water and sediment.

V_* is the shear velocity.

$\frac{V\mu}{\gamma D^2}$ is the ratio of Fr^2/Re which is a ratio of viscous forces to gravitational forces.

$\frac{Sd}{D}$ is the product of $\frac{d}{D}$ and S.

$\frac{V_*d}{\nu}$ is the Reynolds number in terms of the shear velocity and mean diameter of the bed material. This parameter is proportional to the ratio of particle size to the thickness of the laminar sublayer. Specifically, $V_*d/\nu=11.6\ d/\delta'$.

$\frac{V_*}{w}$ is a mobility number of the sediment particle. That is, the ratio of the force producing motion and the force resisting motion of the particle.

$\frac{\tau_0}{\Delta\gamma_s d}$ is the Shields parameter (1936). It is used to indicate the beginning of movement on the bed.

$\frac{V}{V_*}\frac{\tau_0}{\Delta\gamma_s d}$ is the product of the Shields parameter and the velocity ratio $\frac{V}{V_*}$.

$\frac{V}{V_*}\frac{\tau_0}{\Delta\gamma_s}\frac{S}{D}$ is the product of the preceding parameter and $\frac{Sd}{D}$.

These parameters can be introduced into equations 9 or 10.

To determine the dimensionless parameters that are most important in describing $C/\sqrt{g}$ in equation 6, or subsequent equations that evolve from substitutions, an equation involving $(n-k)$ of the dimensionless Pi-terms is selected. Such simplification (like that employed to obtain equations 9 and 10) must be done with considerable care to be sure that important variables are not eliminated. Regardless of the apparent importance or unimportance of the variable at present, it must be remembered that at a later time the variable may prove to be of greater importance than it was initially thought to be.

The various combinations of dimensional and dimensionless parameters deemed significant on the basis of existing concepts, a study of the data collected, and dimensional analysis are related graphically and in many cases by equations, in such a way as to emphasize what variables are of prime importance for evaluating alluvial channel roughness.

Ali and Albertson (1956) simplified (as a first approximation) the dimensional analysis of resistance to flow to the point where three parameters remained.

$$\frac{C}{\sqrt{g}}=\phi_{19}\left[Re, \frac{d}{D}\right] \tag{17}$$

While this is undoubtedly an over simplification of the problem, it serves as a basis from which a first approximation to bed roughness can be made and it emphasizes the effect of Reynolds number. This relationship may be slightly improved, using Laurson's (1958) concept, for the flume data by selecting D/h as an index of roughness in preference to d/D although, considering field application, d/D can be determined more easily than D/h since h is very difficult to measure. The height of roughness h equals d for a plain bed, and height of the ripple, dune, or other form of bed configuration when they exist. In addition, h is a function of the same variables as the roughness and,

577668 O—61——4

thus, is not an independent variable, as directly as is d. However, insight into the problem can be gained by considering the equation

$$\frac{C}{\sqrt{g}}=\phi_{20}\left[Re, \frac{D}{h}\right] \tag{18}$$

It is noteworthy that the variables in equation 18 bear a close resemblance to the variables employed in the diagrams for pipe roughness.

If the methods used to describe resistance to flow in alluvial channels are to be improved, more variables must be considered in the analysis than are considered in equation 17 or equation 18. That is, it seems quite certain that $C/\sqrt{g}$ must vary to a certain extent with more of the geometric characteristics, fluid properties, and sediment characteristics than are indicated in these equations. This is borne out by some of the relations for $C/\sqrt{g}$ developed in the Analysis of Data. For example, in the following equation

$$\frac{C}{\sqrt{g}}=\phi_{21}\left[S, C_D, Re_p, \frac{\rho}{\Delta\rho}\right] \tag{19}$$

most variables have been included and yet accuracy is still inadequate.

Another approach that might further improve the concepts of channel roughness is that $C/\sqrt{g}$ is an additive term. This approach seems logical, especially since total resistance to flow probably consists of surface drag, which is dependent upon the viscous effects as reflected in the Reynolds number; the effect of the sand grains as roughness (form drag); and the effect of ripples and (or) dunes as a form of roughness (form drag). That is, in equation form

$$\frac{C}{\sqrt{g}}=\phi_{22}\left[\text{surface drag, form drag due to grain roughness, form drag due to ripple and (or) dune roughness}\right] \tag{20}$$

The grain roughness is of decreasing importance as the magnitude of the ripples and dunes increases. The drag due to ripples and dunes is usually of minor importance at the beginning of movement, but it increases in importance $\left(\frac{d}{\delta'}<10\right)$ as the size of the ripples and dunes increases until the rapid flow is established. At this point the sand waves develop a plane or a symmetrical pattern of roughness, as shown in figure 23, and there is very little separation and, consequently, only a small amount of form drag. However, there is dissipation of energy in antidune flow from the breaking of the wave. This should decrease the discharge coefficient $C/\sqrt{g}$.

Another factor that may be important, particularly with the rapid flow regime, is that the concentration of sediment being transported is very large on and near the bed, relative to that being transported as suspended load. This is the effect of the density gradient, which Barton and Lin (1955) have related to a special form of the Froude number. Its effect, which is of unknown magnitude, would be to reduce resistance to flow, perhaps in somewhat the same manner as for plug flow in pipes.

In order to describe the types of resistance, considering the foregoing discussion, it would be necessary to know which combination of variables expresses the grain effect and which expresses ripple and dune effect. This accentuates the need for a mathematical model to serve as a guide. Such an equation could help bridge the gap between the empirical treatment and theory. Currently no adequate mathematical treatment has been developed. With progress in experimental research and an improved general understanding of fluid flow phenomena, it is possible that a mathematical model will be developed describing alluvial channel roughness. As an example of correlations involving $C/\sqrt{g}$ as an additive term, refer to figure 26. In this case

$$\frac{C}{\sqrt{g}}=\phi_{23}\left[K_1\left(\frac{V_* d}{\nu}+K_2\right)^n F_r^{\,n}\frac{\Delta\gamma_s d}{\gamma DS}\right] \tag{21}$$

which of the terms in the foregoing equation are related to each type of roughness is still a matter of conjecture. On the basis of the flume data thus far collected, this expression describes $C/\sqrt{g}$ more adequately than any of the preceding relationships.

SUMMARY OF THEORY

Although roughness in alluvial channels has never been described accurately over the complete range of operating conditions, it is quite apparent that in the final analysis $C/\sqrt{g}$, for this flume experiment, must be expressed in such a way that the effect of all the important variables in equation 6 are included over the complete range of operating conditions.

As a final step, assuming that a satisfactory laboratory solution can and will be obtained, it will be necessary to adapt the results to field conditions. This implies that appropriate scale factors must be determined and ultimately the effect of the bank material; the shape of the channel, which is probably a function of the bank and bed material; the bank vegetation; the wind; and the seepage forces should be included, even though it may be virtually impossible to describe some of the effects—for example, the effect of vegetation on resistance to flow—in a precise quantitative manner.

EXPERIMENTAL EQUIPMENT AND PROCEDURE

The establishment of relationships that exist between the resistance to flow in an alluvial channel and the characteristics of the flow and the sediment requires laboratory experiments in which:

1. Uniform steady flow exists. This is only possible in a statistical sense for with a rough movable boundary the velocity is changing both in magnitude and in direction with time and distance. However, just as turbulent flow, with velocity fluctuations, may be considered steady and uniform in a statistical sense, so may flow in alluvial channels. Similarly in terms of scour, the sum of the depositional forces must balance the sum of the aggrading forces. This also is only possible in a statistical sense as the bed at a cross section is continually changing form and the total load fluctuates with time. However, considering a long time average, neither the bed nor the load is changing with time. Possibly equilibrium flow is a more suitable term than steady uniform flow.
2. The variables that describe the flow and sediment characteristics must be measured accurately. The interval of time required to measure precisely a given variable depends upon the variable involved and how it varies with time. To illustrate, a sediment sample should be collected over a relatively long interval of time in order to average its variation with time. Conversely, the point velocities in a vertical should be measured quickly before the bed condition, and consequently, the form of the velocity profile has had an opportunity to change appreciably.

In addition, the scope of the investigation must simulate the conditions found in nature. That is:

1. Various sizes and gradations of bed material that are found in the field must be used, subject to the limitations of the flume.
2. Slope, depth, and water discharge must be varied enough to cover the complete range of field conditions.
3. The effect of temperature variation must be investigated.

Thus far, 45 runs have been completed using one size of bed material with slope, depth, and water discharge varied from run to run. The slope was varied from 0.00014 to 0.01 foot per foot, the discharge was varied from 2 to 21 cubic feet per second, and the flow conditions ranged from no sediment movement to antidune flow. This is, to our knowledge, the first set of data, excluding Gilbert's, that covers this range of conditions.

THE FLUME

The runs were made in a tilting recirculating flume 150 feet long, 8 feet wide, and 2 feet deep as shown in figure 1. The flume is of

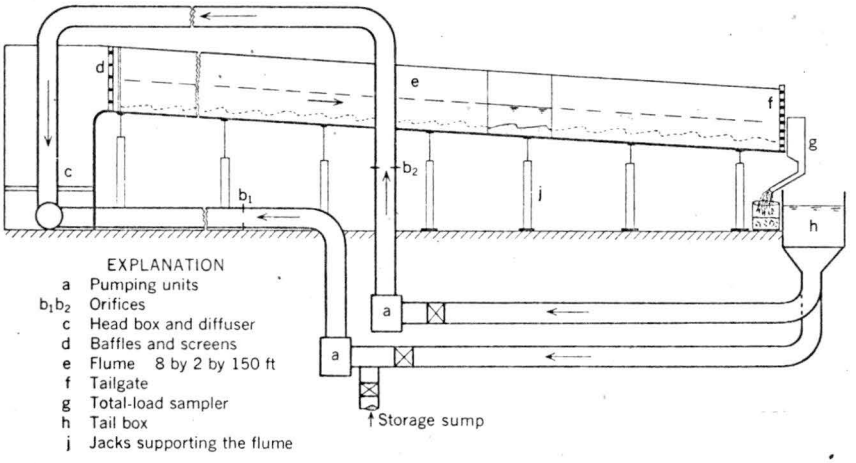

FIGURE 1.—Schematic diagram of the flume.

wood construction resting on steel I-beams. The slope of the flume was changed and adjusted by mechanical jacks placed every 10 feet along the flume. Any slope could be set between the limits of 0 to 0.013 foot per foot. The flume is constructed so that the water-sediment mixture that leaves the flume is returned to the flume entrance by either a 7 cubic feet per second or 14 cubic feet per second centrifical pump (or both). This procedure of recirculating the water-sediment mixture aids in obtaining equilibrium conditions, and in simulating conditions in an infinitely long channel, because the sediment load and size distribution are varied by the flow, rather than by mechanical traps and shakers.

Flow enters the flume through a vertical manifold diffusor, Fiala [3] constructed in the head box. It then flows through a ½-inch wood lattice and a ¼-inch mesh screen. The diffusor and screens effectively distribute the water-sediment mixture and produce a small-scale turbulence that is quickly dissipated. The boundary layer is fully developed for all flow conditions beyond approximately 25 feet downstream from the entrance. This was determined by inspection of the water surface, the bed configuration, and from calculations pertaining to the theoretical boundary layer.

The backwater curve and depth are controlled by a system of vertical notches in which slats are raised or lowered. This method gives precise control of the backwater curve and depth.

ALLUVIAL BED MATERIAL

The flume was filled to a depth of 0.7 feet with a natural river sand. Sand from the Cache La Poudre River was obtained from a com-

[3] Fiala, G. R., 1957. Study of manifold stilling basins, M.S. thesis, Colorado State University, Fort Collins, Colo.

mercial sand and gravel company. The sand was modified by washing and screening to meet specifications. Although it was supposedly free of particles larger than one-fourth inch, a few particles of this size were observed although they were seldom sampled. The sand, principally quartz and feldspar, also contained a small amount of mica. The micaceous particles have a large sieve diameter, but a small fall diameter. That is, they have a smaller settling velocity than a sand particle of the same sieve diameter. The median fall diameter of the bed material is 0.45 mm, based on sample analysis by the visual accumulation apparatus. The size distribution curve for the bed material is given in figure 2.

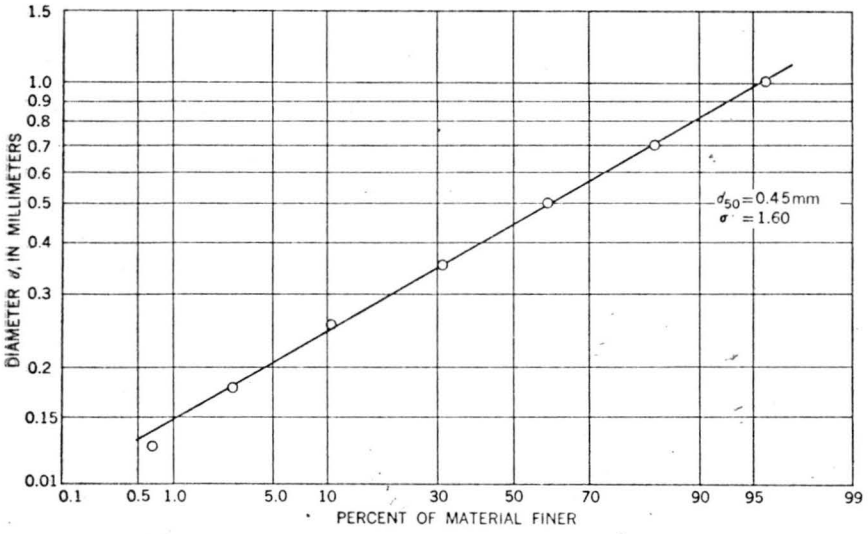

FIGURE 2.—Size distribution curve of the bed material.

The size analysis of the bed material and sediment load were made using the visual accumulation apparatus cited in the foregoing paragraph. It was developed by the Inter-Agency Sediment Project at Minneapolis, Minn. The theory and application of this apparatus were presented in detail by Colby and Christensen (1956).

GENERAL PROCEDURE

The general procedure followed for each run involved recirculating a given discharge of the water-sediment mixture in the flume at a given slope until equilibrium conditions were established.

Only in a general sense were slopes selected. In any flow system where discharge, depth, and slope can be varied, only two of the three variables can be considered as independent. In a natural stream the discharge and slope are normally independent with depth dependent. In the flume the discharge was independent, slope was

independent within limits, and depth was dependent. The slope was preset at the beginning of a run by adjusting the tailgate. Such adjustment indirectly influences the depth as a dependent variable. Generally, and especially at the flatter slopes (0.00014 to 0.0006), the slope of the water surface was adjusted parallel with the bed. With the development of bed configuration, the slope and depth adjusted to the new condition of bed roughness. Thus, for these experiments, the slope and depth are a function of Q and the roughness that develops for that regime of flow. The nonuniformity of flow caused by a change in bed roughness was eliminated by continuing the run until the bed slope and the slope of the water surface again became parallel to each other by natural adjustment of the sand bed.

For tranquil flow the mechanics of establishing the desired slope at the beginning of each run were to set first an M1 backwater curve, and then alternately open the tailgate and measure the water surface slope until the water surface was gradually adjusted to the desired slope. For the flatter slopes, (0.00014 to 0.0006) the bed was carefully screeded to the desired slope before the run. With steeper slopes, since the increased sand movement assisted in obtaining equilibrium conditions quickly, the bed was only raked to remove the dunes from the previous run before starting the new run. In the rapid flow regime the slope was changed by altering the control at the lower end of the flume. The movement of sediment quickly established equilibrium conditions.

Equilibrium flow was considered established if the same bed configuration was established for the full length of the flume, excluding the section influenced by entrance conditions and the water surface slope remained essentially constant with respect to time $\frac{\partial S}{\partial t}=0$.

The time required to establish equilibrium conditions varied with the slope and the discharge. Some runs with flat slopes required 3 and 4 days to achieve equilibrium, whereas, at steeper slopes equilibrium was established in 2 or 3 hours. Every run involved continuous flume operation until it was completed. Whether or not equilibrium conditions were established, in the final analysis, rested on the measured data and the judgment of the experimenter. To insure the achievement of equilibrium conditions most of the experiments were continued longer than the required time as indicated by measurements.

DATA OBTAINED

WATER-SURFACE SLOPE

Water-surface elevations were measured every 5 feet along the flume using a precision level and a Lory point gage. These elevations were plotted on graph paper and an average slope determined. Average

slope of the water surface was determined periodically throughout each run. These slopes were used to establish the water surface slope at equilibrium. The final slope that is used in the analysis of the data was computed by the method of least squares. To measure slopes for those runs in which antidunes formed was difficult because of the rapidly changing water surfaces. Water-surface elevations for these runs were determined by averaging the water-surface elevations taken at an upstream and downstream cross section over a period of time. In addition, the slopes were also determined in the conventional way by taking more time and not measuring the water-surface elevation while antidunes were breaking.

DISCHARGE

To obtain the desired range in discharge, two pumps were used. One, a 12-inch pump with a maximum discharge capacity of 7.98 cubic feet per second and the other, a 15-inch pump with a maximum discharge capacity of 13.38 cubic feet per second. The 12-inch pump was used for runs 1–18, for which $Q<8$ cubic feet per second. For the runs 19–45 inclusive, the 15-inch pump was used for all discharges up to 13.34 cubic feet per second. For $Q>13.34$ cubic feet per second the 12-inch pump was used at its maximum capacity and the discharge from the 15-inch pump was varied to obtain the desired total discharge. Carefully calibrated orifice meters and water-air manometers, read to the nearest one-hundredth of a foot, were used to measure the discharge. The orifice meter for the 12-inch pump is made of stainless steel, is circular, and has a diameter of opening of 10.137 inches. It is located in a vertical section of pipe 10 diameters downstream from the pump and 6 diameters downstream from a right angle bend. The orifice meter for the 15-inch pump consists of a vertical side contraction with stainless steel edge. It is located in a horizontal section of pipe, 11 diameters downstream from a 45° bend, (fig. 1).

Both orifices were calibrated in place. The orifice meter for the small pump was calibrated using a calibrated Cipolletti weir. The orifice meter for the larger pump was calibrated volumetrically.

Water discharge was measured four to five times each day during a run. The average discharge for a run is the mean of these periodic discharge determinations.

WATER TEMPERATURE

Water temperature was measured with a mercury thermometer to the nearest 0.5° C each time the water discharge was determined. The effective temperature recorded for each run is the average of the temperature measurements made after equilibrium conditions were reached.

DEPTH

Depth was determined by three methods. Two of the methods involved the use of the level and point gage, whereas the third method used discharge and average velocity measurements and the continuity equation. Depth was measured directly by the first two methods after the run was completed and the flume drained.

Using the first method, the elevation of the bed was measured along the centerline of the flume at 2- to 5-foot intervals, depending on the bed roughness. From these bed elevations, the average elevation of the reach was computed. The difference between the average bed elevation and the average water-surface elevation is the depth.

Using the second method a reach in the channel, from 2 to 20 feet long, between stations 80 and 105, was carefully screeded. The length of reach used depended on the bed roughness. After screeding, the bed was inundated with water to help attain natural compaction of the bed material. The mean elevation was determined at the center of this screeded section by averaging the elevations for 25 to 60 points located symmetrically in the reach. This average elevation was then subtracted from the corresponding water-surface elevation to determine the average depth.

The third method was to divide the mean water-sediment discharge by the average velocity of the flow as determined from the velocity profiles. That is, $D=A/8=Q/8V_p$ for a nominal width of channel of 8 feet.

The depths as determined by methods 1 and 2 are in good agreement. Five of the runs with the roughest bed configuration had differences in depth of about 0.04 foot. All the other runs had differences less than 0.02 foot. However, the differences between depths determined by averaging bed and water surface elevations (methods 1 and 2) and depths calculated from the velocity profiles and discharge measurements (method 3) were quite large. Some of these differences exceed 0.10 foot. The large difference between depths computed by method 3 and methods 1 and 2 indicate that the velocity profiles obtained in the cross section were not adequate to determine the true average velocity.

MEAN VELOCITY

The mean velocity was computed from the velocity profiles, and the continuity principal, using the depth as computed by methods one or two. In the first case the mean velocity in each of three velocity profiles was calculated and then averaged to determine the mean velocity in the cross section. It was this velocity that was used to determine depth by the third method in the foregoing paragraph. In the second case, the average velocity is $V=Q/8D$ as determined from the continuity equation.

577668 O—61——5

VELOCITY PROFILES

Velocity profiles were obtained by measuring point velocities in the selected verticals with a calibrated pitot tube using a water-air manometer. The pitot tube was calibrated in a towing tank. For slower velocities a tilting manometer which gave a 1×10 magnification of head was used, and for the faster velocities a vertical manometer was used. After equilibrium conditions were established, profiles were taken at 3 to 5 verticals in a cross section with 4 to 12 velocity points in each vertical. The cross sections where velocities were measured were always located between stations 95 and 105.

Velocity profile data at a cross section were determined as rapidly as the pitot tube could stabilize. However, in a run with a dune bed, the dunes would often change the lower part of the profile considerably, especially if measuring was started over a trough and then the crest of a dune moved in where the trough had been before the measurements had been completed. In the regime of flow with antidunes it was virtually impossible to obtain velocity profiles in that part of the flow where the antidune existed. However, velocities above the crest and in the trough of antidunes were determined with the pitot tube, and surface velocities were measured by timing floats through the crests of the antidunes and to the side of the antidunes.

BED MATERIAL

Except for runs 13, 14, 16, 17, and 18, at least four samples of the bed material were taken from the bed at random for each run. The size distribution of each sample of bed material was determined using the visual accumulation tube (VA tube). The VA tube determines the fall diameters.

TOTAL SEDIMENT LOAD

Total load was determined periodically, after equilibrium conditions were established, by using a width-depth integrating total load sampler. A water-sediment sample weighing from 100 to 160 pounds was taken 4 or 5 times during a run. These samples were analyzed and the results were combined to determine total load. The time during which the samples were collected varied from half an hour to 3 hours.

From these samples of the total load, the concentration was determined on a dry-weight basis and the size distribution was determined in terms of fall diameter, using the VA tube. When the amount of sediment in the samples was small, the samples were composited for the size analysis. When the amount of sediment was large, the sam-

ples were combined and then split until reduced to the amount of material that could be analyzed. This sometimes meant four or five splittings. Duplicate analysis of separate portions of the splittings were run through the VA tube apparatus and averaged to establish the size distribution of the total load.

SUSPENDED-SEDIMENT SAMPLES

Suspended-sediment samples were collected at the same cross section as the velocity profile data using the DH–48 hand sampler. Five samples were obtained for each run, using the equal transit rate (ETR) method of sampling. Where the depth was shallow (less than 0.5 foot), the sampler was rocked forward to sample a larger portion of the flow. Some runs were not sampled and for runs 1–6 and 8–18 the suspended load was too small to measure. Concentration and size distribution were determined for the suspended sediment using the same procedure as for total load.

BED CONFIGURATION

The height and length of the ripples, dunes, and antidunes were measured by the point gage. The bed configuration was measured along the center line of the flume over a reach that varied from 20 to 80 feet in length, depending upon the roughness pattern. That is, as the magnitude of roughness increased, the length of reach for which bed configuration was measured was increased.

The bed configuration was always measured after the flume had been drained. However, when standing waves and (or) antidunes existed, the bed configuration was also measured during the run. The elevation of the crest and trough of the water surface with standing waves and (or) antidunes and the corresponding elevation of the bed was measured. Because the bed is extremely firm with this type of flow, the elevation of the bed was accurately determined.

To determine the average length and height of the bed configurations, the bed profile was plotted. The height was computed by summing the vertical distances between the crests and troughs and dividing by the number of these distances. The wave length was computed by dividing the overall flume length, from crest to crest or trough to trough, over which the bed configuration had been measured by the number of dunes or ripples in that length.

In addition to measuring the bed configuration, photographs of the bed were taken for all runs. The velocity of the dune was determined for some of the runs by observing the time of travel of the crest of the dune with respect to a fixed point at the glass window.

PRESENTATION OF DATA

In the foregoing section, descriptions are given of the method of measuring and (or) collecting the data needed to describe the channel geometry and the characteristics of the flow and sediment as they relate to channel roughness. In this section these data will be discussed with respect to their range, variation, and accuracy of measurement.

The basic variables that were recorded for each run are given in table 1 and a discussion of the basic variables follows.

WATER-SURFACE SLOPE

The final water-surface slope based on water-surface elevations measured along the flume and the corresponding coefficient of correlation are given for each run in table 1. The variation of magnitude in slope for the runs ranges from 0.00014 to 0.0101.

The precision with which the water-surface slope determinations were measured is excellent. This is illustrated graphically in figure 3 by plotting water-surface elevations versus distance along the flume for typical runs. The bed roughness for these five runs range from a plane bed with no movement of bed material to antidunes. Note the relatively small amount of scatter about the least-square lines.

DISCHARGE

The average discharge of the water-sediment mixture for each run is given in table 1. The tabulated discharge is the mean of the periodic discharge measurements recorded during a run. The maximum deviation from the average discharge for any one run, as determined from the periodic discharge measurements, is approximately 4 percent. However, in most of the runs the maximum deviation from the mean was less than 2 percent. The magnitude of the discharge ranges from 1.84 to 21.62 cubic feet per second.

The discharge calibration curves for both pumps are well defined, although there is more scatter for the small circular orifice than for the side-contracted orifice. This scatter results from the method of calibration. The maximum deviation of any calibration point from the rating curve in the range of discharge used is 4 percent for the circular and 0.7 percent for the side-contracted orifice.

The maximum change in discharge for each 0.01 foot change in the manometer reading for the entire range of discharge was 2 percent of the discharge for either of the orifices. However, for discharges greater than 2.7 cubic feet per second for the 12-inch pump and 6.0 cubic feet per second for the 15-inch pump, the change in discharge was less than 1 percent.

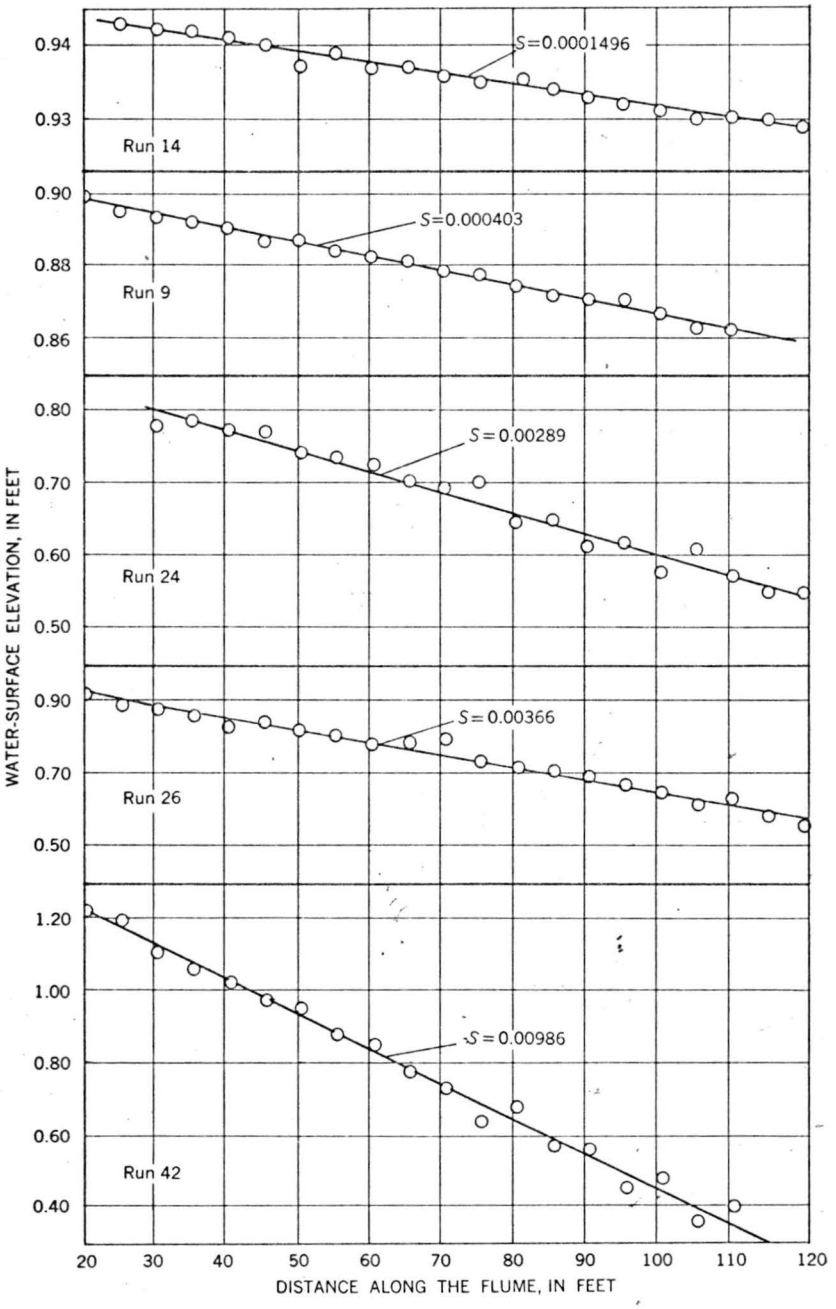

FIGURE 3.—Typical water-surface profiles.

TABLE 1.—*Summary of the data*

Run No.	$S\times10^3$	Q (cfs)	$\nu\times10^5$ (sq ft per sec)	D (ft)	V (ft per sec)	V_p (ft per sec)	T (°C)	Bed material		Total load					Dunes				Bed form
								$d\times10^3$ (ft)	w^1 (fps)	$d\times10^3$ (ft)	σ (0)	w (fps)	Concentration (ppm)	Concentration lbs/sec/ ft$\times10^4$	L (ft)	h^2 (ft)	L/h	D/h^3	
14	0.01469	3.94	1.402	0.611	0.806	0.75	10.2	(4)	0.196	(5)	(5)	(5)	0	0				418.00	Plane bed.
17	.01597	6.22	1.340	.978	.795	.85	12.0	(4)	.202	(5)	(5)	(5)	1	0.49	0.77	0.04	19.25	24.50	Ripples.
16	.01672	5.11	1.340	.812	.786	.85	12.0	(4)	.202	0.728	2.70	0.082	2	.80	.69	.06	11.50	13.50	Do.
13	.01865	1.84	1.460	.353	.652	.57	9.0	(4)	.190	(5)	(5)	(5)	0	0				24.00	Plane bed.
15	.02316	5.07	1.375	.798	.794	.82	11.0	(4)	.190	(5)	(5)	(5)	0	0	(6)	(6)	(6)		Ripples.
18	.03120	3.62	1.363	.584	.775	.72	11.3	(5)	(5)	(5)	(5)	(5)	1	.28	.71	.04	17.75	14.62	Do.
2	.03581	7.90	1.375	.822	1.201	1.20	11.0	1.35	.200	.968	2.47	.118	94	58	1.21	.07	17.29	11.71	Do.
3	.03948	7.90	1.355	.850	1.162	1.27	11.5	1.48	.202	.935	2.79	.116	101	62.2	1.36	.09	15.11	9.45	Do.
9	.04028	3.84	1.340	.549	.874	1.07	12.0	1.54	.202	.361	3.80	.027	2	.60	.73	.06	12.17	9.15	Do.
1	.04186	7.85	1.460	.800	1.227	1.44	9.0	1.44	.190	1.160	3.95	.141	23	14.0	2.00	.10	20.00	8.00	Do.
5	.04676	7.93	1.375	.750	1.322	1.53	11.0	1.52	.200	.863	2.77	.103	26	16.1	1.00	.07	14.29	10.70	Do.
11	.04910	1.95	1.355	.349	.699	.88	11.5	1.46	.202	(5)	(5)	(5)	4	.61	.80	.06	13.33	5.85	Do.
4	.05679	7.94	1.410	.691	1.436	1.67	10.0	1.51	.195	1.030	2.29	.125	92	57.0	4.16	.15	27.73	4.60	Dunes.
8	.05974	3.83	1.340	.513	.933	1.11	12.0	1.39	.202	.846	2.78	.100	8	2.39	.73	.06	12.17	8.60	Ripples.
7	.07772	7.98	1.355	.699	1.427	1.61	11.5	1.46	.202	.637	3.36	.068	268	167	4.41	.20	22.05	3.50	Dunes.
10	.08760	1.95	1.390	.327	.746	.93	10.5	1.54	.197	1.400	1.64	.190	20	3.04	.83	.08	10.38	4.15	Ripples.
6	.08844	3.90	1.430	.456	1.069	1.14	9.5	1.64	.192	1.440	1.86	.189	42	12.8	1.56	.10	15.60	4.55	Do.
12	.10560	1.95	1.349	.288	.847	1.12	11.7	1.54	.202	.771	3.70	.089	1	.15	.89	.06	14.83	4.85	Do.
19	.11160	4.24	1.140	.406	1.305	1.41	18.0	1.57	.213	.951	3.28	.126	208	68.8	6.42	.26	24.69	1.57	Dunes.
21	.11410	12.12	1.200	.958	1.581	1.44	16.0	1.36	.208	.820	2.81	.102	641	606	4.82	.31	15.55	3.10	Do.
22	.12450	13.54	1.209	.996	1.699	1.66	15.7	1.25	.207	.791	2.58	.097	710	750	7.50	.52	14.53	1.92	Do.
25	.18880	4.91	1.170	.417	1.472	1.84	17.0	1.50	.210	1.100	2.03	.148	378	145	6.29	.26	24.19	1.61	Do.
20	.19260	8.14	1.188	.606	1.679	1.68	16.4	1.61	.210	.663	2.84	.077	508	323	5.37	.36	14.92	1.68	Do.
23	.24660	13.34	1.200	.649	2.569	2.54	16.0	1.40	.208	.755	2.43	.092	856	891	6.60	.41	16.10	1.58	Do.
24	.28860	8.73	1.170	.620	1.760	2.24	17.0	1.23	.210	.820	2.29	.103	1200	817	5.51	.31	17.77	2.00	Do.
40	.30100	21.41	1.110	.807	3.316	3.30	19.0	1.41	.215	.810	1.97	.105	2460	4110	7.35	.31	23.71	2.60	Do.
39	.36380	20.64	1.110	.548	4.708	4.60	19.0	1.51	.215	1.010	1.92	.138	3960	6380	3.68	.10	36.80	376.00	Standing wave.
26	.36580	14.45	1.170	.336	5.376	3.84	17.0	1.54	.210	1.140	1.87	.154	4580	5160				229.00	Plane bed.
28	.36580	11.19	1.200	.397	3.523	3.77	16.0	1.65	.208	1.110	1.84	.151	4230	3690	2.57	.05	51.40	7.90	Standing wave.
29	.36880	4.54	1.158	.300	1.892	2.25	17.4	1.48	.212	1.190	2.08	.164	1850	655	6.40	.23	27.83	1.30	Transition.[6]
31	.43220	14.85	1.155	.438	4.238	4.08	17.5	1.58	.212	1.250	1.80	.174	4750	5500	3.16	.06	52.67	302.00	Standing wave.
27	.43540	7.91	1.140	.331	2.987	2.84	18.0	1.66	.213	1.210	1.98	.171	4100	2530	10.22	.19	53.79	1.73	Do.
36	.44600	3.15	1.110	.193	2.040	1.94	19.0	1.50	.215	1.350	2.10	.194	1370	337	.93	.03	31.00	7.50	Transition.[6]
41	.46600	21.62	1.119	.535	5.051	4.88	18.7	1.14	.214	1.380	1.76	.200	4340	7320	3.93	.14	28.07	365.00	Standing wave.
30	.49230	5.33	1.164	.270	2.468	2.62	17.2	1.57	.210	1.350	1.85	.190	3550	1480	6.02	.12	50.17	2.25	Transition.[6]
35	.49400	5.58	1.170	.249	2.801	2.75	17.0	1.48	.210	1.330	1.71	.189	4610	2010	2.20	.07	30.20	171.00	Do.
34	.54580	8.44	1.155	.283	3.728	3.68	17.5	1.31	.212	1.450	1.77	.213	5690	3750	2.46	.08	30.78	196.00	Standing wave.
33	.60660	10.02	1.200	.272	4.605	3.80	16.0	1.26	.208	1.360	1.85	.190	6810	5320	2.76	.10	27.60	185.00	Do.
38	.61900	21.38	1.110	.497	5.377	5.29	19.0	1.36	.215	1.590	1.83	.233	6230	10390	3.81	.09	42.33	342.00	Do.
37	.62000	18.87	1.125	.426	5.537	4.98	18.5	1.65	.214	1.740	1.83	.256	5570	8200	3.82	.08	47.75	291.00	Do.

32	.65580	14.96	1.140	.372	5.027	4.65	18.0	1.35	.213	1.67	1.84	.246	6180	7210	3.71	.29	12.79	253.00	Antidune.
45	.86200	5.58	1.113	.279	2.500	3.36	18.9	1.33	.215	1.59	1.61	.236	9630	4190	1.59	.11	14.45	154.00	Do.
44	.89800	10.83	1.098	.283	4.783	4.76	19.4	1.74	.218	1.57	1.60	.233	15100	12750	2.95	.21	14.05	195.00	Do.
42	.98600	13.43	1.082	.313	5.363	4.97	20.0	1.30	.220	1.72	1.65	.262	11400	11940	3.62	.25	14.08	216.00	Do.
43	1.01000	21.42	1.125	.433	6.184	------	18.5	1.57	.214	1.28	1.80	.180	11500	19210	5.81	.27	20.03	298.00	Do.

[1] Computed on basis of average median diameter (0.00148 ft) and water temperature for the run.
[2] h is the median diameter of the bed material when a plain bed or antidune regime exists.
[3] 3-dimensional flow.
[4] No sample.
[5] No size analysis.
[6] Dunes not measured.

DEPTH OF FLOW

The average depth recorded in table 1 was obtained by the screeding method described in the preceding section (method 2). This procedure gives better results with fewer bed elevation determinations than are required when working with the undisturbed bed. That is, relatively speaking, the average elevation of a plane can be described more accurately with fewer readings than are required to describe the average elevation of an active stream bed when there are dunes and potholes that are sometimes of the same order of magnitude as the depth. Screeding the bed was done with care since any disturbance, such as that caused by walking on the bed, changed the degree of compaction of the bed material, and hence its average elevation and the average depth. To offset this danger, the bed was first carefully screeded without increasing the compaction and then flooded to achieve natural conditions before taking elevation measurements.

Another possible source of error always present is the degree of compaction of the bed material, which varies with the form of the bed roughness. For instance, a bed with dunes and potholes is fairly loose prior to draining the flume as compared to its conditioning after drainage. This problem of changing density could be avoided, as well as the problem of the erosion of the roughness pattern caused by draining the flume, if a suitable means of measuring bed elevation during the run could be found.

KINEMATIC VISCOSITY

The kinematic viscosities are given in table 1 and are based on the temperature of the water during the runs. In the runs, the temperature varied from 9° C to 20° C, which resulted in a range in kinematic viscosity of 1.082 to 1.46×10^{-5} square feet per second.

The recorded temperature for each run is the average of the water temperatures obtained after equilibrium was established. The maximum deviation from the recorded temperature during any individual run was approximately 1° C. This magnitude of temperature fluctuation changes the kinematic viscosity about 3 percent.

MEAN VELOCITY

The mean velocity V, used in the computation of parameters was obtained by dividing the discharge by the product of the width of the flume times the average depth. The velocity thus accumulates the errors inherent in depth and discharge calculations. The errors in discharge and depth may be additive or compensating in their effect on the velocity. The velocity, as determined by the continuity principal, is given in table 1. Also included in table 1 is the mean velocity, V_P as determined from the velocity profiles.

VELOCITY PROFILES

Typical velocity profiles are given in figure 4. This figure illustrates the form of the distribution curves of the velocities on semilogarithmic paper for a plane bed with no movement, run 14, for a bed covered with ripples, run 9, for a bed covered with a fully formed dune pattern, runs 21 and 24, for a plane bed with $Fr>1$, run 26, and for antidune flow, run 44. The stations given in the figure locate the velocity profiles in the transverse direction. The zero station in the traverse direction was at the right edge of the flume.

Velocity profiles in an alluvial stream are continually changing in form. For example, the lower part of the velocity profile is considerably different when taken at the crest of the dune than when taken in the trough where a separation zone exists. In the separation zone, the direction of flow is reversed. For flow with standing waves

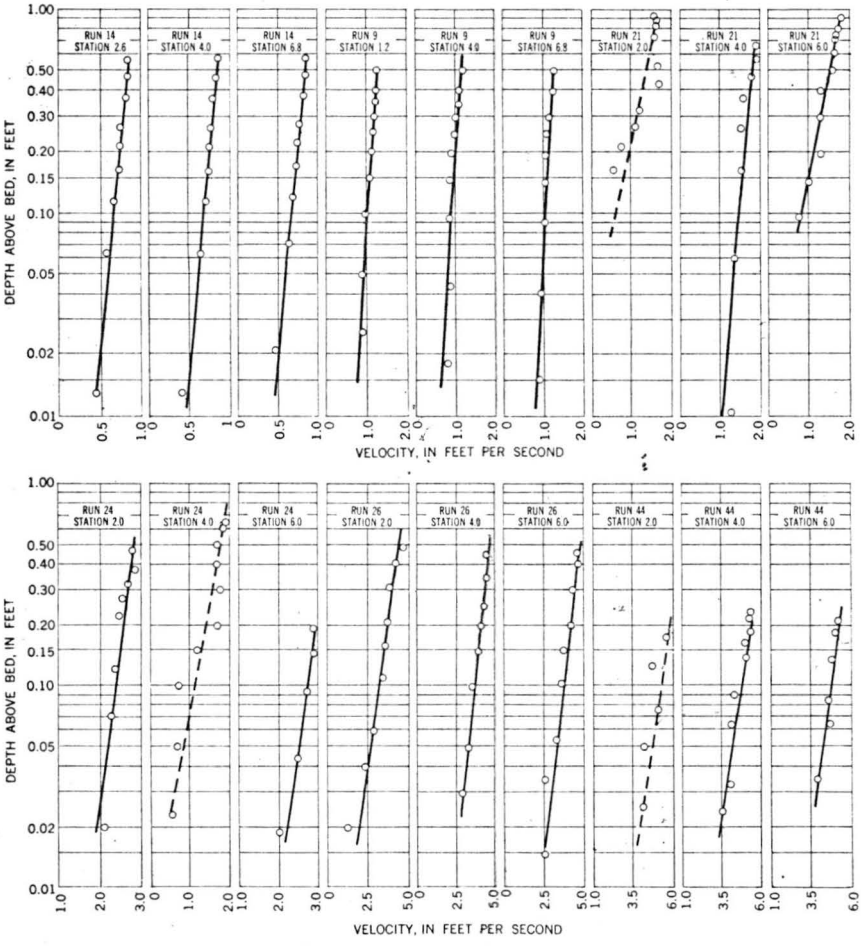

FIGURE 4.—Typical vertical velocity distribution curves at different stations across the flume.

577668 O—61——6

and antidunes, the velocity profile in the vertical is considerably different through the trough than through the crest. In addition, the velocity of this type of flow at any point changes so rapidly that the profile is constantly changing.

BED MATERIAL

The median fall diameter d, the nondimensional standard deviation σ, and the fall velocity w of the median diameter of the bed material as determined from the samples for each run are given in table 1.

The median fall diameter of the bed material d for each run was determined from size distribution curves plotted on log-probability paper. The standard deviation σ of the bed material for each run was calculated from the equation

$$\sigma=1/2\left[\frac{d}{d_{16}}+\frac{d_{84}}{d}\right] \tag{24}$$

in which

d_{16} is the size of the material for which 16 percent is smaller.

d_{84} is the size of the material for which 84 percent is smaller.

These sizes were obtained directly from the size distribution curves for each run.

The median fall diameter of the bed material used to calculate parameters was obtained by averaging all of the data for size analysis and plotting the results to obtain the composite size distribution curve given in figure 2. This was done because the probability is small that any single sample or small group of samples will give the size distribution of a natural unsorted sand. The more samples that are analyzed the greater the probability of obtaining the actual size distribution. The possibility that the characteristics of the bed material change with time was investigated by taking the size distribution, as determined from samples from the first 18 runs, and comparing it with the size distribution for the last 26 runs. There is very little difference between the two, which is an indication that the sand size was not changing as a result of abrasion and there is no appreciable selective sorting of certain sediment sizes.

Using the data shown in figure 2, the median fall diameter, as determined from all the samples, is 0.45 mm or 0.00148 foot, and the relative standard deviation is 1.60. Statistically there are 99 chances in 100 that this median diameter is within 4 percent of the true median diameter of the bed material.

The fall velocity of the bed material, which is given in table 1, is based on the average median fall diameter (0.45 mm), shown in figure 2, and the temperature of the water for the run in question.

This fall velocity was determined using the graph on page 41 of Inter-Agency Report No. 4 (1941).

TOTAL SEDIMENT LOAD

The median fall diameter, the standard deviation, the fall velocity of the median diameter, the concentration of the total load, and the computed total sediment load for each run are given in table 1. The methods used to determine size, relative standard deviation, and fall velocity were similar to those used to establish these values for bed material. The total load was computed by multiplying the concentration by the discharge and a constant to convert to the units of pounds per second per foot of width.

The median diameter of the particles in the total load varied from 0.000361 to 0.00174 foot. In certain runs the median diameter d for the total load was slightly larger than the median diameter of the particles in the bed. This may have been due to segregation of the bed material and possibly error in sampling and analysis. In other runs the d for the total load was smaller than the d for the bed material. To a limited extent, this may be due to some sampling error, but it is largely caused by the transport capacity being proportionately smaller for certain sizes than their proportionate availability in the bed. Beyond a certain limiting bed shear, however, the d for the total load should be equal to the d for the bed material.

The concentration of the total load varied from 0 to 15,100 ppm which gave a total load variation from 0 to 1.28 pounds per second per foot.

Samples had to be taken over a time long enough to average the effects of storage in the dunes and the resulting fluctuations in concentration passing the samplers. A short sampling time resulted in concentration data that were usually either too high or too low, and size distributions that were either coarser or finer than they should have been. This may explain the smaller total load and finer size distributions for runs 20–24, 39, 40, and the coarser size distribution for runs 6 and 10. However, the sampling times for run 20 were long enough for the dunes to move a distance equal to four times their length, and for the dunes corresponding to the other runs to move a distance at least equal to their length. This indicates that the sampling time was long enough and that the finer size distribution resulted from storage of certain sizes of bed material in the dune. However, larger samples collected over a longer time should be obtained with the rougher beds.

SUSPENDED SEDIMENT

The concentration of suspended sediment varied from 0 to 14,500 ppm. There were some concentrations of suspended sediment that

were larger than the concentrations of total load. This is a physical impossibility considering average values and illustrates the inadequacy of the method of sampling. The greatest difficulty occurred when the bed was extremely rough and (or) the depth of flow was quite shallow, and it is attributed to positioning the nozzle of the hand sampler too close to the bed. Suspended sediment is not included in the tabulation of concentrations.

BED CONFIGURATION

The geometry of the bed is described by the spacing and height of the sand waves, the ratio of length to height of the sand waves, the ratio of depth of flow to height of sand waves, and the form of the bed configuration for each run, which are all given in table 1.

It is difficult to measure the bed configuration accurately, as in the measurement of depth, because the accuracy depends upon the effects on the original configuration of stopping the flow and draining the flume, and upon the number of bed configuration measurements taken.

It was necessary to exercise care in stopping a run so that a wave would not be created that would alter the bed roughness as the wave traveled up the flume, and in draining the flume so that the roughness pattern would not be eroded. In the tranquil flow regime it was possible to stop the flow and drain the flume without appreciably altering the bed configuration. However, with steeper slopes (rapid flow regime) this was not possible.

OBSERVED FLOW PHENOMENA

The form of bed roughness in alluvial channels is a function of the sediment characteristics and the characteristics of the flow. That is, the bed configuration may be changed by changing either discharge (which effects the depth), slope, temperature, or the median diameter or size distribution of the bed material. In the flume experiments the bed material was not changed and the slope, temperature, and depth were varied. Under these conditions the following forms of bed roughness were observed:

Tranquil-flow regime:

1. Plane bed without movement,
2. Ripples,
3. Dunes,
4. Transition from dunes to rapid-flow forms.

Rapid-flow regime:

5. Plane bed with movement,
6. Standing sand waves,
7. Antidunes.

The major forms of bed roughness are sketched in figure 5.

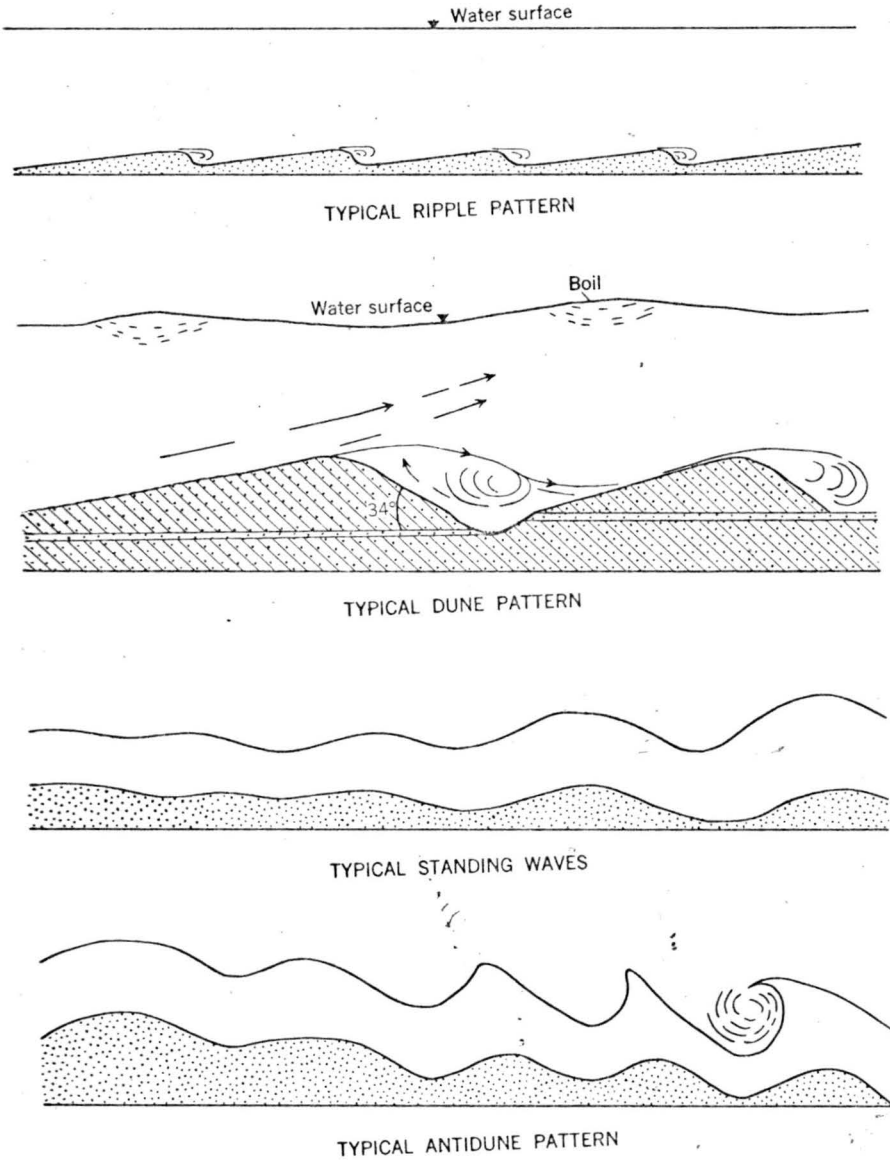

FIGURE 5.—Major forms of bed roughness.

Slope and size of bed material are the dominant parameters that determine what form of bed configuration will occur, although, with slope and bed material size constant, the form of the bed may be changed by varying depth (changing Q) or changing temperature. However, changing depth or temperature will not change the flow regime from tranquil to rapid unless the slope for a given size of bed material is close to the critical slope. That is, for a given size of bed

material with a small slope and the dune bed form of roughness, it is impossible to create the standing wave form of roughness by changing depth or temperature. With a given depth and temperature, all bed forms can be created by changing slope when using a sand size bed material. This last statement has to be qualified because three-dimensional flow will occur in shallow depths and with it occur multiple bed roughness forms. It is possible to have a size of bed material that will prevent formation of some of the bed forms regardless of the depth, slope or water temperature. Figure 28 in the section Analysis of Data illustrates the effects of temperature, slope, depth, and size of material on the forms of bed roughness.

For a given size of bed material the change from one bed form to another is not necessarily abrupt. Neither does it occur at the same slope (depth and temperature held constant) nor the same depth (slope and temperature held constant), if the change in bed form is reversed. That is, the change of bed form from ripples to dunes may occur at a different slope (depth and temperature held constant) than the reversed change from dunes to ripples. This gradual change and (or) hysteresis effect result in a transition from one bed form to another. This transition of bed forms is of major importance when the flow changes from tranquil to rapid, or from rapid to tranquil, that is, when the bed form changed from dunes to standing sand waves with standing water waves or to a plane bed with a plane water surface, or when it changes from standing sand waves to dunes. The change in flow regime from tranquil to rapid or from rapid to tranquil may, if conditions are right, occur in a natural river. That is, if the slope of the energy grade line is close to the critical slope, a change in the stage of the river could result in a change in the flow regime. Tranquil flow exists at low stage and rapid flow exists at high stage. With a change in regime there would be a break in the discharge rating curve for that stream. Because there is a hysteresis in the transition from rapid flow to tranquil or from tranquil flow to rapid, the point at which the break in the discharge rating curve would occur depends on whether the stage is rising or falling and also on the rate of change.

It is important to note that the velocity of the flow in an alluvial channel is not zero at the bed. The velocity of the water through the bed is slow but important, especially when considering seepage force. The velocity of this flow in the bed is highest in the dune bed form, since the porosity of the material is high, and smallest in the rapid flow regime, where the bed material is closely packed. In the flume, as a result of the effects of the floor, the velocity of the flow through the bed was probably lower than in most natural streams, and consequently, the seepage force was lower. In a natural stream the velocity

in addition to being greater in the direction of flow, has vertical components in the bed resulting from inflow or outflow. This inflow or outflow, which depends on the water table of the surrounding area, causes large seepage forces. These forces may have a considerable effect on the form of bed roughness and transport of sediment.

BED FORMS IN THE TRANQUIL-FLOW REGIME

PLANE BED WITHOUT MOVEMENT

The plane bed with no movement of bed material was soft and easily disturbed. Figure 6 is a photograph of a plane bed. This bed was photographed through the water during the run. The word "plane"

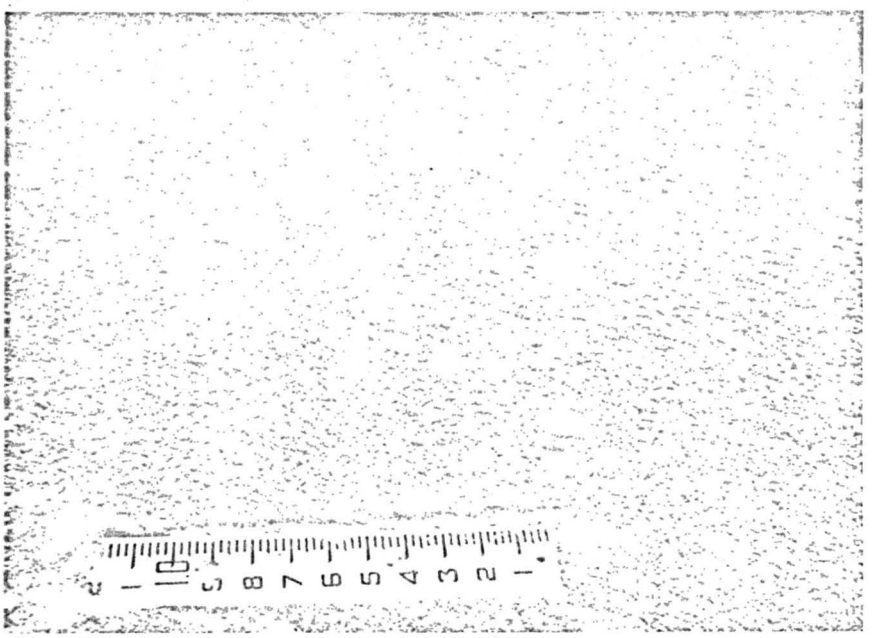

FIGURE 6.—View of bed with no sediment movement. Water-surface slope $S=0.000147$ (run 14).

is used to emphasize that the surface of the bed was not hydraulically smooth. That is, for a smooth, rigid hydraulic boundary the magnitude of d/δ' must be such that $d/\delta'<0.25$. The minimum d/δ' for the flume runs was 0.40. Obviously it is possible to obtain a hydraulically smooth boundary without bed movement by decreasing the slope or the depth. However, obtaining a smooth bed or a plane bed without sediment movement in itself has little practical importance. The important thing to consider is the point at which movement of bed material will begin as the slope or depth, or both, are increased. It is interesting to note that the point where movement begins, for this size of bed material, is not the point where a transition from the hy-

RIPPLES

The form of the ripples is illustrated in figure 5, and a photograph of typical ripple formation is shown in figure 7. The height of the ripples was less than 0.10 foot and their longitudinal spacing was less than 2.0 feet. Their length-height ratio, L/h, varied from 10 to 20. The ratio of depth of flow to ripple height ranged from 4 to 24; Manning n ranged from 0.019 to 0.027; and $C/\sqrt{g}$ ranged from 7.8 to 12.4. The upper limit of n-values, and the lower limit of $C/\sqrt{g}$, in general, were associated with the shallower depths.

There was little or no suspended sediment movement with the ripple bed form. The water was sufficiently clear so that the bed was visible at all times. The total sediment load ranged from 1 ppm to 101 ppm and the sediment moved in more or less continuous contact with the bed, rolling up over the crest of the ripples and coming to rest on its forward slope. The sediment on the forward slope did not move again until it was exposed in the upstream part of the ripple as the ripple migrated downstream. Thus the movement of the sediment particles takes place in steps. The length of the step and time interval between steps depends on the length of the ripple and the ripple velocity.

Beds with ripples were soft, but not as soft as those with dunes. The water surface was very smooth with little visible difference from the water surface for a plane bed without movement. The separation zone

FIGURE 7.—View upstream of ripple configuration. Water-surface slope S=0.000403 (run 9).

downstream from the crest of the ripple is such that there was little evidence of jet impingement on the downstream ripple. The reverse flow in the trough moved only the finest mica particles and the turbulence was small at the interface between the main current and the separation zone.

As the slope and (or) depth were increased beyond a certain limit, the ripples were modified and the appearance of the bed changed. Compare the ripples shown in figure 7 with the dunes in figure 8.

FIGURE 8.—View upstream of dune configuration. Water-surface slope $S=0.00247$ (run 23).

The bed changed from the ripple pattern to a dune pattern when the slope and (or) depth were changed such that d/δ' was approximately 1.0. The Froude number was approximately 0.28. This change was abrupt and the dunes established themselves over the full length of the flume in a matter of hours. To change from dunes to ripples (Q=constant) it was necessary to decrease the slope and increase depth from those values at which ripples changed to dunes. Because of the reduced transport capacity caused by decreasing slope and increasing depth, considerable time is required for the flow to convert a dune configuration to ripples.

DUNES

The form of the dunes is illustrated in figure 5 and a photograph of typical dunes is shown in figures 8 and 10. In this sequence of runs, dunes ranged in average height from 0.15 to 0.52 feet and in

length from 4.0 to 7.5 feet. The length-to-height ratio, L/h, varied from 14 to 28. The ratio of depth of flow to dune height, D/h, ranged from 1.5 to 5.0. The Froude number varied from 0.38 to 0.60 with 0.60 fixing the upper limit of the dune bed form. The Manning n varied from 0.018 to 0.032, although from observations of the bed, much larger values of Manning n would be expected (figs. 8, 9, and 10). The reason for these smaller n-values is that in a flume this large, as in a natural stream, the dunes form a pattern that allows part of the flow to sideslip or bypass the dune. This sideslippage or meandering of the flow around the dunes is very obvious when a smaller discharge is run over a dune bed formed by a larger discharge.

Dunes move downstream as a result of sediment toppling over the crest and accumulating on the downstream face of the dune. The larger the amplitude of the dune the more sediment is stored in the dune and the lower the dune velocity. Smaller dunes with their higher velocities overtake the larger dunes. This results in a much larger dune and decreases the dune velocity. Velocity of the dunes varied from 0.03 to 0.70 feet per minute. The higher dune velocities were associated with the steeper slopes and shallower depths. Conversely, the larger dunes were associated with flatter slopes and deeper depths.

The L/h ratios for dunes and ripples are similar. The ratios ranged from 10 to 24 for ripples and 14 to 28 for dunes. This indicates that

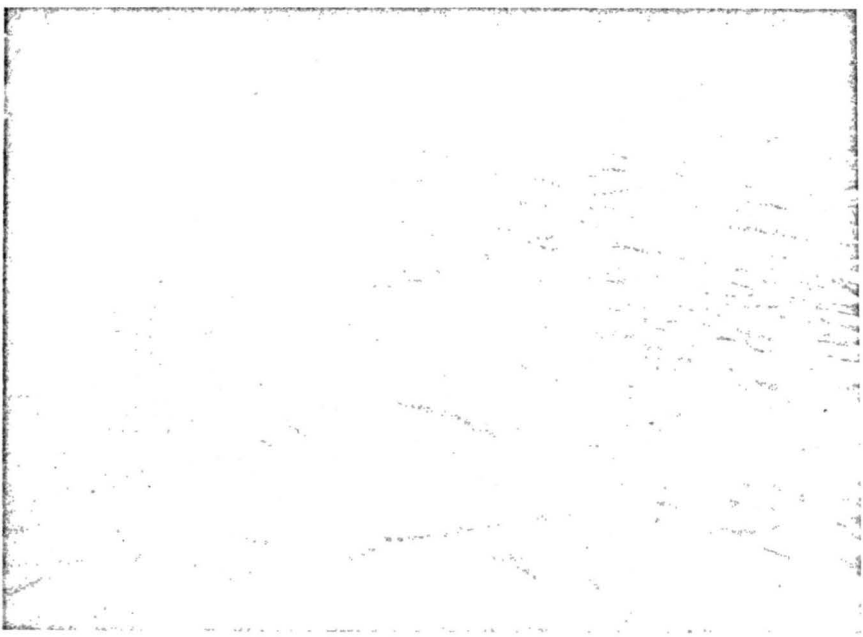

FIGURE 9.—Flow over dune configuration similar to that shown in figure 10.

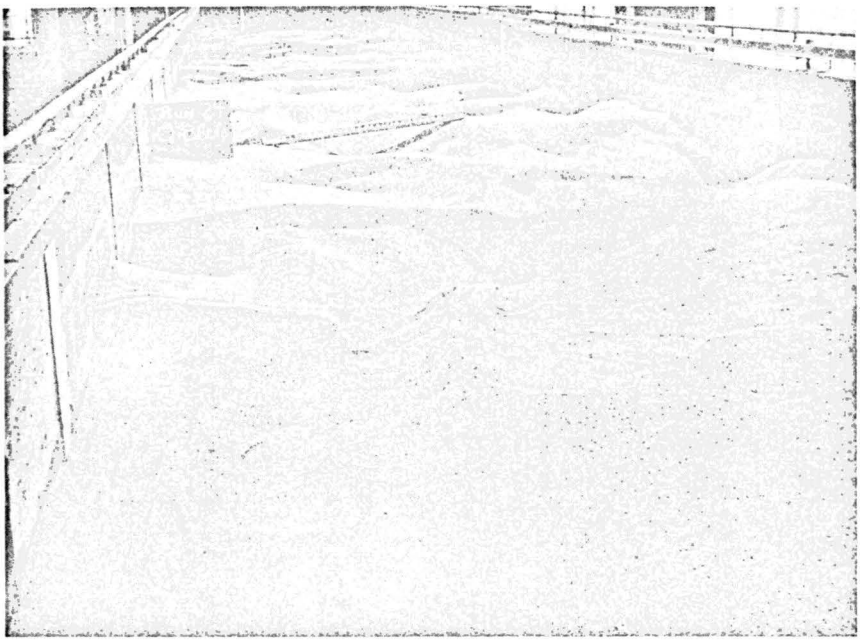

FIGURE 10.—View upstream of dune configuration. Water-surface slope $S=0.00289$ (run 24).

there is a correlation between dune height and dune length for a given sediment. That is, if the height of the dune or ripple increases with change in slope or depth, the length also increases. The variation in the L/h ratios may be the result of the randomness of the dune configuration, making it difficult to obtain true average length or height. Some of the variation in the L/h ratios may result from including the separation zone in the measured lengths of the dune. That is, the true length of the dune may extend from the end of the separation zone to the downstream crest. The measured length as used, however, was from crest to crest. The magnitude of the separation zone increases as slope increases.

The ratio of depth of flow to dune height, or relative roughness D/h, was different for ripples from that for dunes. Ripples had a larger D/h ratio than dunes. This parameter may help explain why the n values were smaller for ripples than for dunes. Also for the ripple and dune bed form, the larger n values occurred with the smaller D/h values.

It seems from the flume data that maximum dune height, during two-dimensional flow, is limited by the depth of flow. The dune will only grow until its crest is within a certain distance from the water surface, unless three-dimensional flow exists. Also, with a given slope and continuously increasing depth, the dune height may reach some maximum value for that size of sediment and water temperature,

and increasing the depth beyond this limiting depth will not increase the dune height. If this is true, then in order to predict accurately the resistance to flow in an alluvial channel, the point where dune height becomes independent of depth must be determined. This point may be a function of the width of the channel. If dune height becomes independent of depth, the n-values may decrease with stage. That is, h/D, the relative roughness, will decrease.

The bed with dunes is very soft and fluid, and there is considerable segregation of the bed material. The upstream slope and crest of the dune, which has a slope of approximately 2 to 4 degrees, consists of the fine and coarse material moving downstream. This slope of the upstream face is practically the same as that for the upstream face of the ripples. On the upstream face of the dune, at the lower slopes, ripples form. At the higher slopes these ripples on the dunes are not apparent. The downstream face, which has a slope between 31 and 39 degrees, consists of the coarser fraction of the bed material. This coarser fraction is the material that can not be swept into suspension at the crest but topples over the crest and avalanches down the foreslope. It is this avalanching that results in the soft nature of a dune bed. The material is deposited by the force of gravity and has relatively large voids. If it were deposited by the dynamic force of the fluid it would be packed into place, with a relatively small voids ratio. Bagnold (1941, p. 238–240) observed and explained the same phenomena in wind blown dunes. The trough of the dune contains a layer one eighth to 2 inches thick of the fine material from the bed. Part of the fines in the trough comes from the sediment that is swept from the crest and part comes from the lower part of the upstream face of the downstream dune, where the main current that overrides the separation zone impinges on the bed (fig. 5). As the water-surface slope is increased over the dune form of bed roughness, the toe of the downstream dune is more actively blasted and eaten away by the water with high velocity that impinges on it. This is an additional source of fine material that is deposited in the trough by the reverse flow in the separation zone. Velocities as high as 1.3 feet per second in the upstream direction were measured in the separation zone.

The slope of the downstream face of the dune, which varied from 31° to 39° with an average of 34°, was clearly defined by lines formed by the dark colored mica particles as the dune moved downstream (fig. 5). The angle of repose in air for dry noncohesive sand 1 mm in diameter (95 percent of the bed material in the flume was finer than 1 mm) varies from 29° to 32° depending on angularity of the particles (Simons and Albertson, 1960). That is, well rounded 1 mm particles have an angle of repose of 29° and very angular particles have an angle of 32°. It is probable that the angle of the forward face of the

dune is increased above the angle of repose of dry sand in air as a result of the increase in pressure in the separation zone on the foreplane of the dune and as a result of the reverse flow in the trough moving up the face of the dune. This is verified by the fact that, as the velocity of flow was reduced to zero in the flume, the face of the crest of the dune slumped, reducing the angle of inclination of the face.

With the dune form of bed roughness the water surface is uneven and turbulent (see fig. 9). Over the crest of the dune, the water surface is lower than over the trough. This is the result of the acceleration and deceleration of the flow as it contracts over the crest and expands over the trough. This was illustrated for rigid boundaries by Rouse (1946 p. 135 and 139). The degree of roughness (turbulence) of the water surface increases with an increase of bed roughness. The roughest water surface occurred where there were large water-surface boils. These boils stood approximately one-tenth of a foot above the surrounding water surface. However, the roughness of the water surface was not great enough to affect the determination of the water-surface slope (fig. 3). The turbulence created at the interface between the main flow and the flow in the separation zone dissipated considerable energy, and normally the disturbance caused by the interference was visible on the water surface downstream. In the dune bed form, the suspended sediment concentration, the intensity of the turbulence, the relative roughness, and the velocity of the reversed flow in the trough all increased with increasing slope. Along with the dunes, potholes formed that had a depth equal to the height of the dunes. These, as well as the dunes, caused boils on the water surface, which were evident downstream from the dunes. The potholes and boils moved downstream in front of the dunes at the same velocity as the dunes. There were normally from 10 to 20 potholes and boils evident in the full length of the flume for this type of bed roughness. The potholes appeared to develop as a result of the increased strength of the secondary circulation in the separation zone. The combination of the velocity in the direction of flow and the secondary circulation causes a spiral circulation similar to that in a whirlwind. This rotating motion scours out additional material at a point in the separation zone and produces a pothole. The existence of dunes and potholes is indicated visibly by the formation of very strong boils that transport considerable suspended sediment upward to the water surface.

This segregation of the material by the formation and movement of dunes means that a large number of bed material samples must be obtained and analyzed before the size distribution can be accurately established. For this flume material, 60 samples were needed before another sample would not alter the median diameter by a significant

amount. This segregation should have some value, though, because in a natural stream where $Fr<0.6$ it might be possible to determine the characteristics of the bed roughness by taking core samples of the bed, conditions permitting.

TRANSITION FROM DUNES TO RAPID-FLOW FORMS

The change from dunes to rapid flow forms is complex and the form of the bed roughness is erratic. With small changes in depth and (or) slope the bed configuration may change from a form typical of dunes to a form typical of rapid flow or some combination of the two. The transition occurs when the depth and (or) slope are changed to give $d/\delta'>2$ and $0.6<Fr<1.0$.

There is a definite break in the Froude number when changing from dunes to rapid flow forms. For flow with dunes the maximum Froude number was 0.60. Obviously, the minimum Froude number is 1.0 for rapid flow. Runs with a Froude number between 0.6 and 1.0 showed a multiple roughness. That is, the bed form was in between dunes and a plane bed and consisted of washed out dunes and sand bars.

It is logical that the upper limit of the Froude number, for the dune bed form, is considerably less than 1.0. The change in roughness, and consequently the change in resistance to flow, and the dissipation of energy are large when changing from the plane bed or undulating bed during rapid flow to dunes, whereas the change in energy for changes in the Froude number in the vicinity of $Fr=1$ is small. Thus, the velocity and depth, when the bed form changes, are changed considerably, resulting in a low Froude number. Conversely, the change from dunes to rapid flow forms results in smaller loss of energy because of the reduced roughness, resulting in higher velocities, low depths and Froude numbers ≥ 1.0.

There is a hysteresis effect in the change of bed roughness from dunes to rapid flow forms and back to dunes. The value of slope and (or) depth for the change depends on the bed configuration prior to the change. If the bed is covered with dunes, a slope of 0.0035 may be required before rapid flow will occur and the dune configuration is destroyed. If the bed is plane, the slope may be decreased to 0.0025 before the flow will change from rapid to tranquil and dunes will form. This hysteresis effect may be attributed to the change in energy with a change in flow regime from tranquil to rapid, or from rapid to tranquil. That is, a change from potential to kinetic energy with a change from tranquil to rapid flow or change from kinetic to potential energy with a change from rapid to tranquil flow. This change in energy results from the large change in roughness associated with the change in flow from tranquil to rapid or from rapid to tranquil. The

Manning n values for dunes range from 0.018 to 0.032, whereas, with rapid flow, Manning n values range from 0.010 to 0.015.

The fact that, for this bed material, a typical dune pattern did not occur with a Froude number equal to or greater than 0.60 is important, especially if it holds true for other bed materials. Runs 40 and 29 had Froude numbers equal to or slightly greater than 0.60. Their bed forms were washed-out dunes with rather large L/h ratios. The Manning n values were 0.018 and 0.021 respectively, which are small when compared with n values for dunes, but are higher than rapid-flow n values. It seems that the magnitude of Manning n increases as the percent of the area of the bed that is covered with dunes decreases.

Three other runs (30, 35, 36) with $0.6<Fr<1.0$ had long, low bars diagonal to the flow. These bars were 20 to 30 feet in length with L/h ratios between 30 and 50.

Runs 29, 30, 35, and 36 had distinctly different types of flow occurring side by side (fig. 11 and 12). This three-dimensional flow was probably caused by using discharges that were too small with respect to slope. This phenomena was also observed where the antidune bed forms existed and the discharge was decreased beyond a given value (run 45). For three-dimensional flow the n values ranged from 0.014 to 0.023, whereas the n values for standing waves was approximately 0.012.

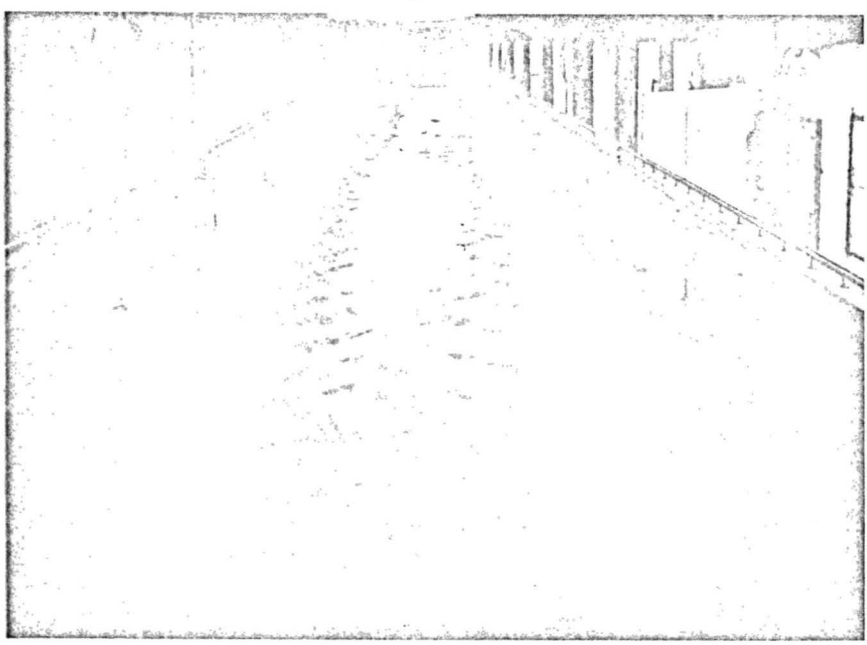

FIGURE 11.—Three-dimensional flow over the sandbar configuration of figure 12 (run 35).

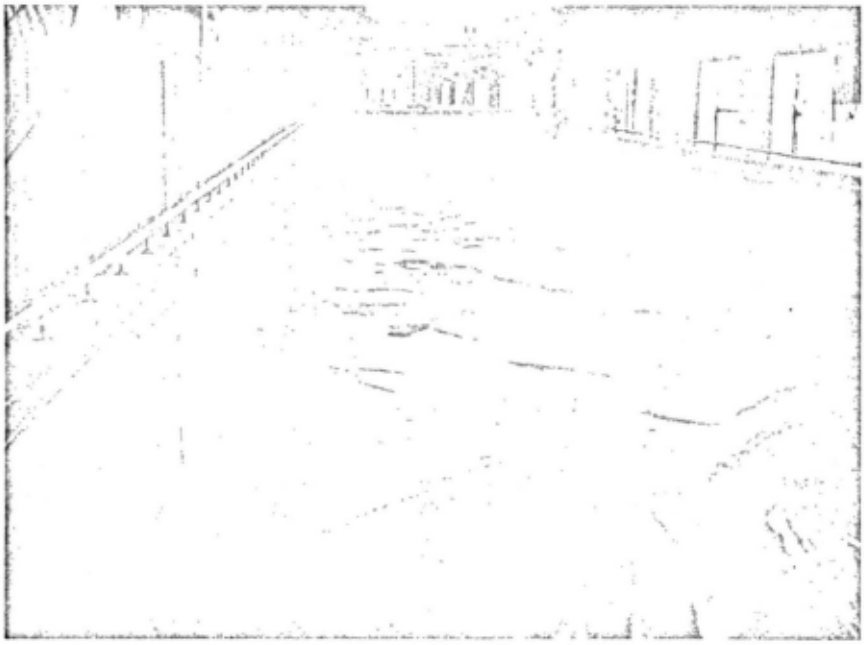

FIGURE 12.—View upstream of sandbar configuration. Water-surface slope $S=0.00494$ (run 35).

Three-dimensional flow probably results because discharge and slope were controlled in the experiments, and with the steeper slopes the small discharges set up conditions favorable for three-dimensional flow. Other experimenters may have observed this flow condition because of the limited discharge capacity of their flume system and the resultant large width-to-depth ratio that develops as slope is increased. In runs with the dune bed form, the smallest discharge was sufficient to insure two-dimensional flow. Presumably, however, by further decreasing the discharge, three-dimensional flow could also occur in runs with the dune bed form.

Runs 29, 30, 35, and 36 were discounted in analysis of data because they were three-dimensional.

BED FORMS IN THE RAPID-FLOW REGIME

PLANE BED WITH MOVEMENT

In runs with rapid flow ($Fr>1.0$), three forms of sand bed surfaces and water surfaces were observed: plane bed and water surface, standing sand and water waves, and antidunes.

A completely plane bed with a plane water surface over the full length of the flume was only produced once in all the runs (fig. 13). It was anticipated from a study of the existing literature that this would be the most common type of bed configuration between dunes and antidunes. Most experimenters have recorded a large number

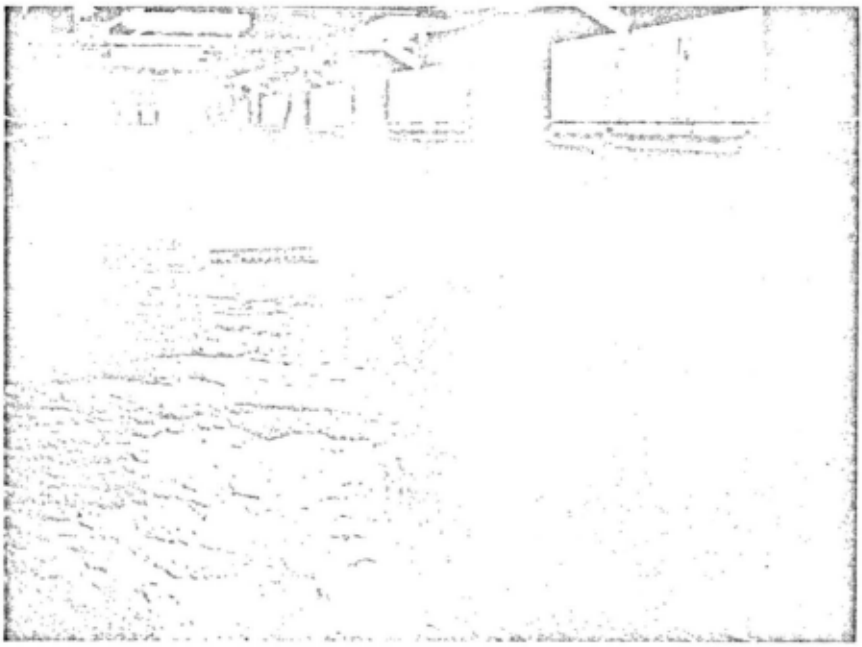

FIGURE 13.—View upstream of a plane bed during rapid flow. Water-surface slope S=0.00366 (run 26)

of runs with plane beds, particularly when they worked with short flumes. In many of the runs in this study, there was a plane bed surface and plane water surface for the first 60 to 70 feet of the flume, but beyond that point standing waves developed. Laursen (1958), in his experiment using a flume 105 feet long and 3 feet wide, also reported difficulty in obtaining a plane bed. Perhaps plane beds result from using flumes with insufficient length for standing waves or antidunes to form.

For the plane bed of figure 13 the Manning n value is extremely small (n=0.0078); the total sediment load is large (4,580 parts per million); the Froude number is 1.6; and the d/δ' value is only 2.1. This Froude number is the next to largest recorded even though the slope for this run was not as great as for the runs in the antidune regime. The sand bed was very firm.

STANDING WAVES

The water surface consisted of symmetrical standing waves of low amplitude, (fig. 14). The standing waves formed and gradually disappeared but unlike antidunes they had no tendency to break or migrate upstream. The forms of bed roughness observed with standing waves, in the order of increasing slope, were a diagonal dune pattern cross-laced like a shoe string (fig. 15), a plane bed, (fig. 13),

FIGURE 14.—View downstream of standing wave during rapid flow. Water-surface slope $S=0.00364$ (run 39).

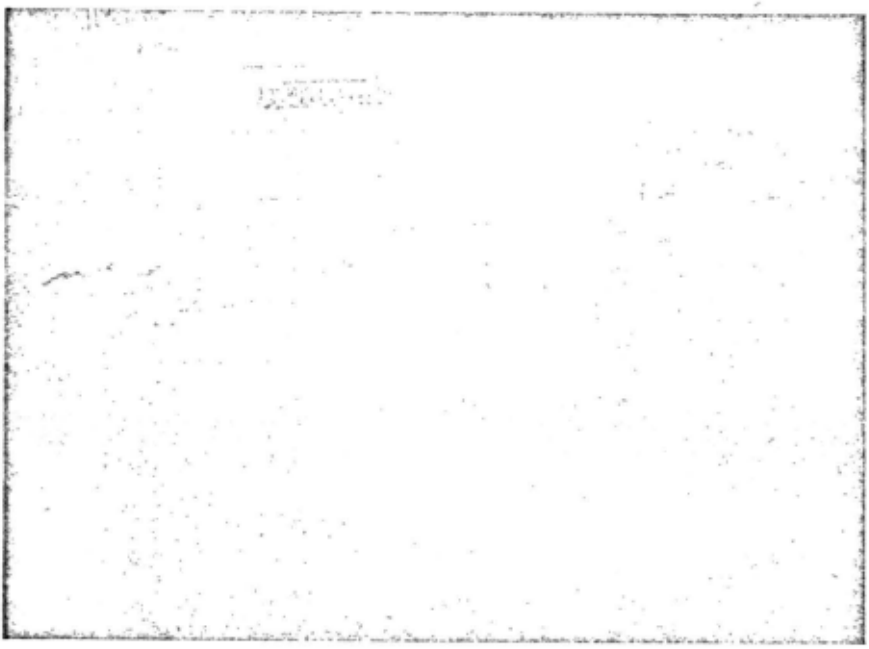

FIGURE 15.—View of cross-laced configuration looking upstream. Water-surface slope $S=0.00435$ (run 27).

and a symmetrical, undulating sand wave similar in form to those observed in the antidune regime.

The standing water waves formed when Froude number was approximately 1.0. The standing water waves with the diagonal cross-laced sand bars shown in figure 5 formed with this lower Froude number. The standing water waves on a plane bed formed at a Froude number of about 1.1, and standing water waves on a bed with undulating sand waves formed when $1.2<Fr<1.5$. The Manning n for the standing sand wave bed form is relatively small, ranging from 0.012 to 0.015. The water surface waves are 1.5 times as high as the corresponding sand waves. Concurrent measurements of the sand bed waves and the water-surface waves are illustrated in figure 21.

ANTIDUNES

When the Froude number, computed on the basis of average velocity and average depth, was greater than 1.5 and d/δ' was greater than 3.0, antidunes formed.

Antidunes are defined as a train of symmetrical sand waves, inphase with a corresponding train of symmetrical water-surface waves. Both trains of waves move upstream and grow in height until they break (figs. 16–20), resulting in a cyclical fluctuation of the water-

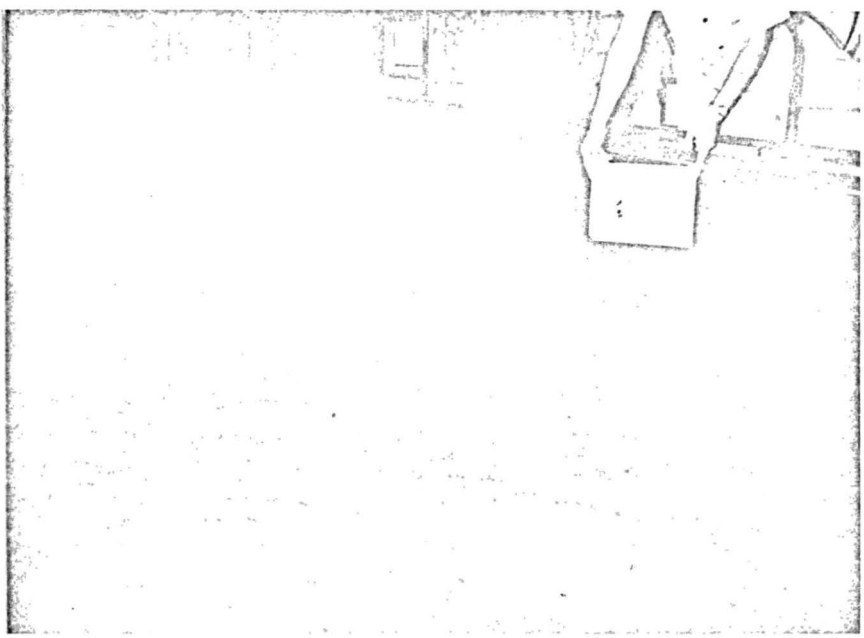

FIGURE 16.—Water surface before antidune wave starts to build up. View is upstream. Water-surface slope $S=0.00986$ (run 42).

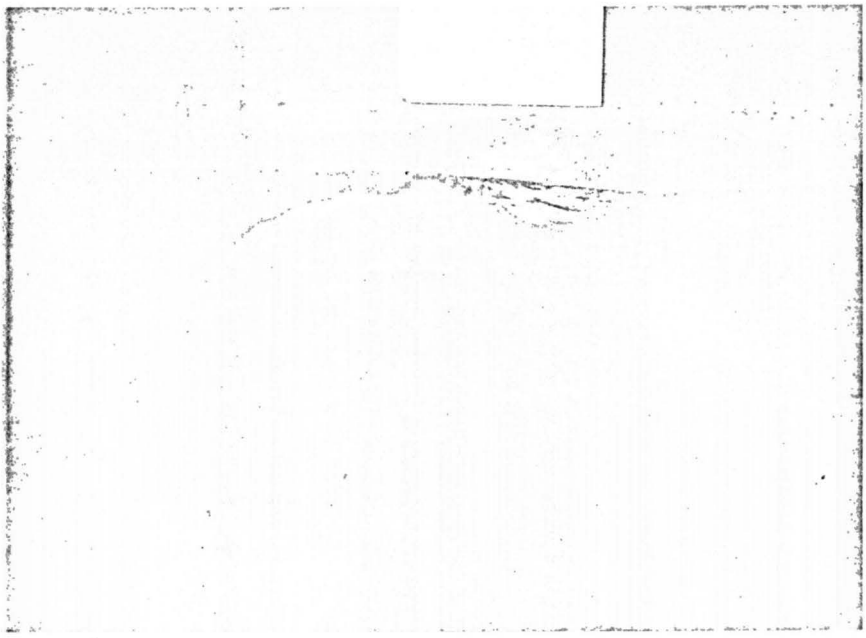

FIGURE 17.—View across the flow at an antidune wave that is forming.

FIGURE 18.—View upstream of an antidune wave at point of breaking.

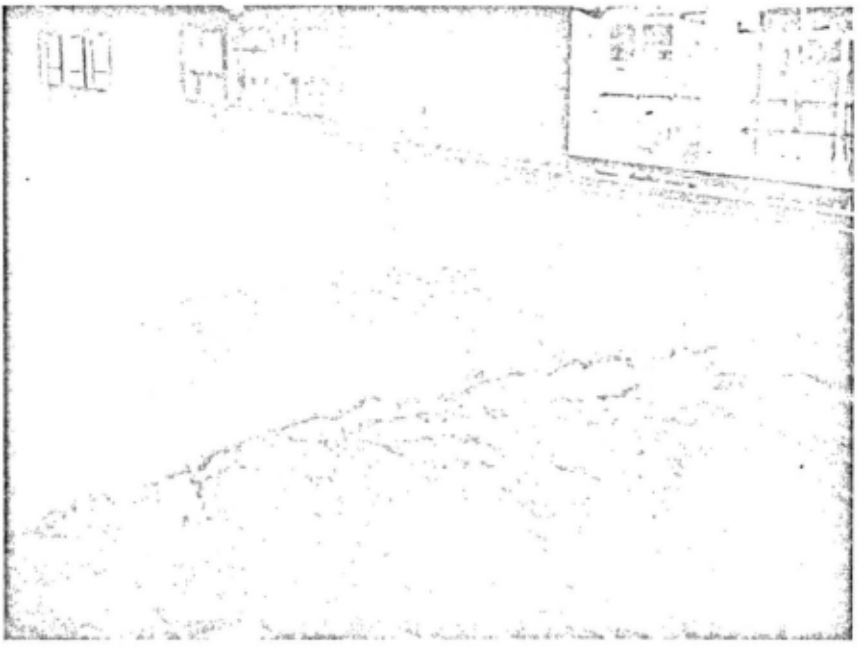

FIGURE 19.—Antidune wave after breaking (run 42).

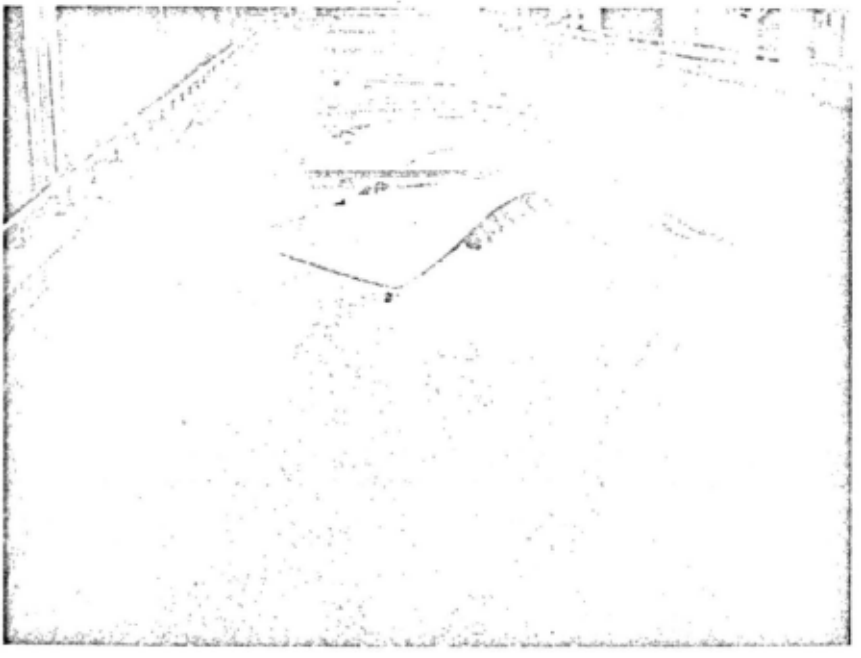

FIGURE 20.—View of bed configuration after antidune flow. The pattern has been somewhat altered by draining the flume.

surface waves and the sand waves. The waves build up from a plane bed with a plane water surface. They grow and move upstream until one or two of the waves become unstable and break as shown in figures 18 and 19. Normally, when one wave breaks, other waves break immediately thereafter for a distance of one or two waves upstream and 4 or 5 waves downstream. That is, depending on discharge and slope, from 1 to 8 waves at a spacing of 1 to 6 feet usually break within a short time interval. This chain reaction that follows the breaking of the first wave is apparently triggered by the action of the first wave that breaks.

In making concurrent measurements of the bed and water surfaces in the troughs and crests of antidunes, it was observed that antidunes become unstable and break when the water surface in the trough of the wave train is approximately the same elevation as the crest of the downstream bed wave (fig. 21). The measurements also indicated that the water waves are 1.7 times larger in amplitude than the corresponding sand waves. The total height of the water-surface waves from trough to crest was from 1.0 to 1.5 times the average depth. When the waves started to break, their heights were about twice the average depth. The breaking of the waves is very spectacular. There is considerable turbulence, dissipation of energy, and mixing of the flow. When they break they sound like the surf in the ocean and there is probably some resemblance, in that the ocean wave, as it climbs the sloping beach, also builds up to an unstable height before breaking.

When the antidunes are building up, the bed is very firm and there is no separation between the flow and bed. However, when the antidune breaks, the crest of the sand wave becomes soft and fluid and seems almost to explode. When the water waves break, the flow is very turbulent; there is separation, and considerable sediment is thrown into suspension. Normally, most of the sediment load is moved as contact load. Total load concentration is very high, ranging from 4,240 to 15,000 ppm for these runs. It appears that the movement of the antidunes upstream results from scour on the downstream side of one sand wave and deposition on the upstream side of the adjacent wave and consequently, the wave moves upstream.

Except for run 45, which was considered three-dimensional, there was only one train of waves in the cross section. The train of waves was located off center at about the left ⅓-point in the cross section. In subsequent runs, however, two trains of waves symmetrically located in the flume were observed several times. The wave train was not continuous throughout the entire length of the flume. That is, a train of antidunes would build up and break in one 20- to 40-foot length of flume and then repeat in another 20- to 40-foot reach, or

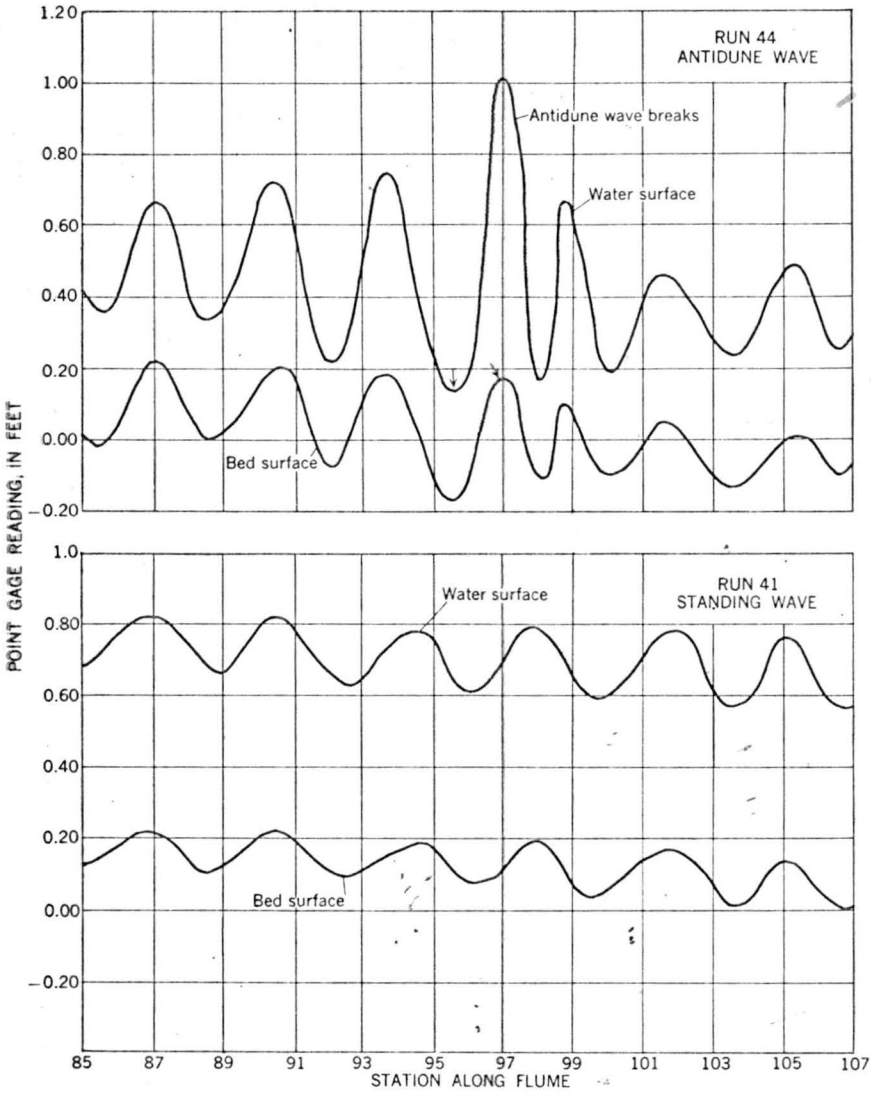

FIGURE 21.—Profiles of the actual water surface and bed configuration for runs 44 and 41. Note: arrows indicating the point in run 44 where the elevation of the crest of the bed surface is greater than the elevation of the trough of the water surface.

they would build up and break in two or three discontinuous lengths of the flume. The building up and breaking, in the different reaches of the flume, might be in phase or out of phase.

The period of time it took for one antidune wave to build up and break, and the number of antidune waves built up at one time varied with the slope and the discharge. During run 32 only one train of six to eight antidune waves would build up and break at a given time. This train of waves, with a total length of about 40 feet, would build

up in, for example, the lower section, then next in the middle or upper sections, and again in the original position. Normally, about two complete cycles occurred every hour (a cycle includes starting with a plane surface, the building up of waves, the breaking of the waves, and the return to a plane surface). For other runs with steeper slopes there were three or four reaches in the flume where the train of waves built up and broke in phase and out of phase, almost continuously.

When the antidunes break, a considerable amount of water is stored in the flume. Observations at the glass-walled section of the flume show that when an antidune breaks, the water and sediment in the wave crest ceases to move or moves upstream until the breaking wave vanishes and then normal flow is restored. At the higher slopes (run 43), when three or four series of antidune waves in the train would build up and break simultaneously, so much water was stored in the flume that the pumps would surge. In the extreme case, antidune waves would build up and break in phase with the surging of the pumps. This resulted in a fluctuating discharge and an increase in antidune activity. So much water was stored in the full length of the flume as a result of the more violent antidune action, that the tailwater level in the tailbox dropped until the pumps lost their prime. To eliminate this degree of surging of the pumps, the level of the water in the sump was raised and more water was continuously added to the sump to replace that stored in the flume. When the antidunes were not breaking, there was a surplus of water, which was discharged through an overflow at the top of the sump.

The storage of water caused by the breaking of the antidune waves probably explains the surging discharge observed in alluvial streams with steep slopes. That is, the antidunes store and release water in the upper reaches of the stream in a random, haphazard manner, but as the flow travels downstream this storage and release of storage causes the antidunes to break in a more systematic pattern until surges develop that cause the antidunes to form and break at regular time intervals. Some field examples of surging flow are Muddy Creek near Pavillion, Wyo., and Medano Creek in the Great Sand Dune National Monument, Colo.

Antidune flow, in terms of fluid mechanics, is very efficient. That is, the Manning n ranges from 0.010 to 0.013. Even though the breaking of the antidunes dissipates considerable energy, the length of flume that this breaking occupies is small in comparison with the total flume length and the period of time the breaking waves exists is small in comparison with the total time for one antidune cycle. This explains the low n values. It was observed that as the antidune activity increased with an increase in slope there was a larger dissipation of energy with a decrease in discharge coefficient $C/\sqrt{g}$ and an increase in

Manning n. Surface velocity measurements, obtained by timing floats along a centerline of a train of antidune waves (when they were not breaking) and along a nearby parallel line where the water surface was smooth, showed that the surface velocity was greater in the train of waves. The velocity in the trough of the antidune is considerably greater than that in the crest. It is possible that the antidunes break when the velocity and depth over the crest decrease because of increasing wave height until a Froude number less than 1.0 results.

The standing wave and the antidune wave may be compared to the flow regimes of rigid boundary hydraulics illustrated by Rouse (1946). The crisscrossed bed pattern (figs. 15 and 20) that is observed with both standing wave and antidune flow resembles the shock waves that form with rapid flow ($Fr>1.0$) in rigid boundaries.

ANALYSIS OF DATA

The basic data (table 1, p. 30) have been utilized as dictated by the investigations of others, by various concepts (many of which are partly intuitive) and the dimensional analysis of the channel roughness problem to obtain the relationships presented in this section. It should also be borne in mind that these relations, excluding figure 28, are based on only one group of flume data, and that the size and gradation of bed material remained constant except as altered by miscellaneous sorting, which may or may not be of significance. That is, d and σ are constant, and w varied only because of temperature changes. The relations presented in this chapter are given in a logical sequence that can be subdivided into four major phases.

1. Relations of a simple nature that illustrate the interrelationship of the variables, geometric variables, the form of bed roughness, and the regimes of flow.
2. Relations of a more complex nature that include the variation of the Manning n, tractive force and total sediment load concentration.
3. Relations that involve roughness in alluvial channels. These relations vary from simple to complex.
4. A plot that utilizes data from both the laboratory and the field to expand the usefulness of the foregoing concepts and to accentuate the existence of two regimes of flow and six major forms of bed roughness.

Appreciable insight of the scope of the data collected, and into the interrelationships of flow to geometric variables can be gained by considering a few simple dimensional plots.

VARIATION OF VELOCITY WITH DEPTH

The variation of velocity with depth and their relations to the six major forms of bed roughness are shown in figure 22. In this and subsequent plots the following notation is used to signify the two regimes of flow and six forms of bed roughness: Tranquil flow—P_1, is plane bed and water surface with no bed movement; R, is ripples;

with rapid flow. Runs of this type plot just below the critical velocity curve. The lines dividing the plot into forms of bed roughness are based on the observed roughness and the Froude number, Fr.

A similar relation, that of D to Q, can be plotted using slope and forms of bed rougness as the other variables. As in the preceding figure, the transition runs will plot just below the critical depth curve.

VARIATION OF TOTAL SEDIMENT-LOAD CONCENTRATION AND MANNING n

Values of Manning n range from 0.008 to 0.032. These n values have been corrected for side effect in accordance with the procedure presented by Einstein and Barbarassa (1951). The magnitude of n_b increases with increasing V until the regime of flow shifts from the tranquil regime to the rapid flow regime where the n's reduce suddenly to approximately 0.012. Undoubtedly, a better relationship of the foregoing type could be obtained by relating Manning n or some other measure of channel roughness with suspended sediment load, except that in shallow depths it is difficult to sample suspended sediment load with significant accuracy. More often than is desirable, when taking the suspended sediment sample, part of the bed material load and in some cases even a part of a ripple or dune may be intercepted, particularly when the velocity is relatively large.

By relating the concentration C_T and the Manning n to the regimes of flow these significant conclusions can be reached.

1. As the flow is increased and the bed changes from a plane bed with no movement to one with ripples, the Manning n increases from about $n=0.015$ to $n=0.025$ with no significant discontinuities.
2. As dunes form a marked increase in Manning n occurs, from $n=0.025$ to $n=0.033$. This increase in n is caused by the large size of the dunes at a spacing conducive to maximum roughness.
3. In the transition from tranquil flow to rapid flow, the resistance to flow is also in transition. It shifts with a small change in depth and slope from high resistance, almost as high as for the dunes, to low resistance, which is not quite as low as for rapid flow. The amount of the resistance to the flow is dependent on the area of the bed covered by dunes.
4. In the rapid flow regime there is a significant decrease in Manning n. This large decrease in resistance to flow can be attributed to the change from dunes to symmetrical sand waves. Dunes have a large separation zone with large form drag, whereas the symmetrical sand wave has no separation zone and has only the form drag resulting from the particle. Possibly some of this decrease in Manning n can be attributed to the movement of large quantities of sediment as bed load. The turbulence

created is insufficient to hold large quantities of sediment in suspension. Consequently, the sediment load that was carried in suspension when dunes formed now is carried near the bed. This heavy concentration, in turn, markedly changes the properties of the fluid-sediment mixture, which means that the fluid is no longer homogeneous. A sort of stratified flow results that inhibits mixing, and the effective bed roughness is extremely reduced. The flow has some similarity to plug flow in pipes. For the single run with $n=0.0078$ the bed was plane, and the resistance caused by the standing waves was not in effect. Under these conditions the similarity to plug flow is even more pronounced.

5. The largest concentration of total load for standing wave roughness occur just before these waves begin to move upstream as antidunes. With antidunes the C_T values are even larger. The same large concentration of sediment exists near the bed as under standing wave conditions, except for the short time while the antidunes are breaking, and hence the Manning n remains small, $0.011<n<0.015$.

VARIATION OF TRACTIVE FORCE AND TOTAL SEDIMENT LOAD

Figure 23 is obtained by plotting the tractive force τ_0, which has been calculated by the equation

$$\tau_0=\gamma DS \tag{25}$$

with the total sediment load concentration in parts per million. Although there is appreciable scatter, a trend definitely exists. That is, the magnitude of total load C_T increases with increasing magnitude of tractive force τ_0. Each run in figure 23 has been labeled in accordance with its form of bed roughness. Using this notation the regimes of flow and forms of bed roughness have been indicated. There is a definite tendency, in this case, for the tranquil flow runs to separate from the rapid flow runs because of the large tractive force associated with runs that have large dunes on the bed.

The deviation of the runs that form dunes from the general trend is a result of an increase in shear τ_0, due to the large size of the dunes, without a corresponding increase in concentration C_T. It is significant that a sudden decrease in τ_0 occurs at about $C_T=2{,}000$ parts per million as the bed changes from dunes to plane bed or standing waves. This is caused by a reduction in roughness, which also decreases the ability of the flow to transport sediment. Consequently, C_T is cut in half from run 40 to run 36, beyond which point C_T, in the transition from dunes to rapid flow bed forms, steadily increases. No such discontinuity occurs at the change from ripples to dunes or at the

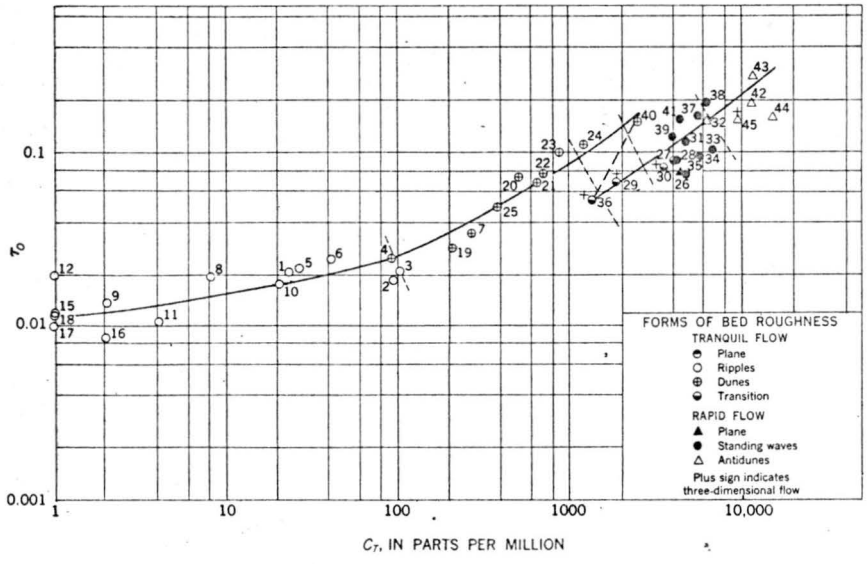

FIGURE 23.—Variation of shear τ_0 and concentration of total load C_T, in parts per million.

change from standing waves to antidunes. There is, however, considerable scatter in the values for the rapid flow regime, which shows that another variable is needed to describe the phenomenon more completely.

RESISTENCE TO FLOW RELATIONS

Working more directly toward the evaluation of variable bed roughness in alluvial channels, and using $C/\sqrt{g}$ as the index of roughness, the applicability of the following equation, suggested by Ali and Albertson (1956), was investigated.

$$\frac{C}{\sqrt{g}}=\phi\left[\frac{D}{d}Re\right] \tag{26}$$

Certain trends were apparent involving these three parameters but there was excessive scatter. It may be that the collection of additional data will improve this condition. Certainly the data presented by Ali and Albertson show that the foregoing functional relationship has merit and warrants additional consideration.

Applying an approach suggested by Liu (1957), the relationship between V_*d/ν and $V\tau_0/V_*(\Delta\gamma_s)d$, for ripple formation, was investigated for both regimes of flow (fig. 24) by using form of bed roughness as the third variable.

It is important to note how precisely the equation

$$\frac{V}{V_*}\frac{\tau_0}{(\Delta\gamma_s)d}=\phi\left(\frac{V_*d}{\nu}\right) \tag{27}$$

describes all forms of bed roughness. These data plot as a curve on log-log paper.

The foregoing curve is of such a nature that it can be modified by adding a constant to the ordinate term to yield two lines that are

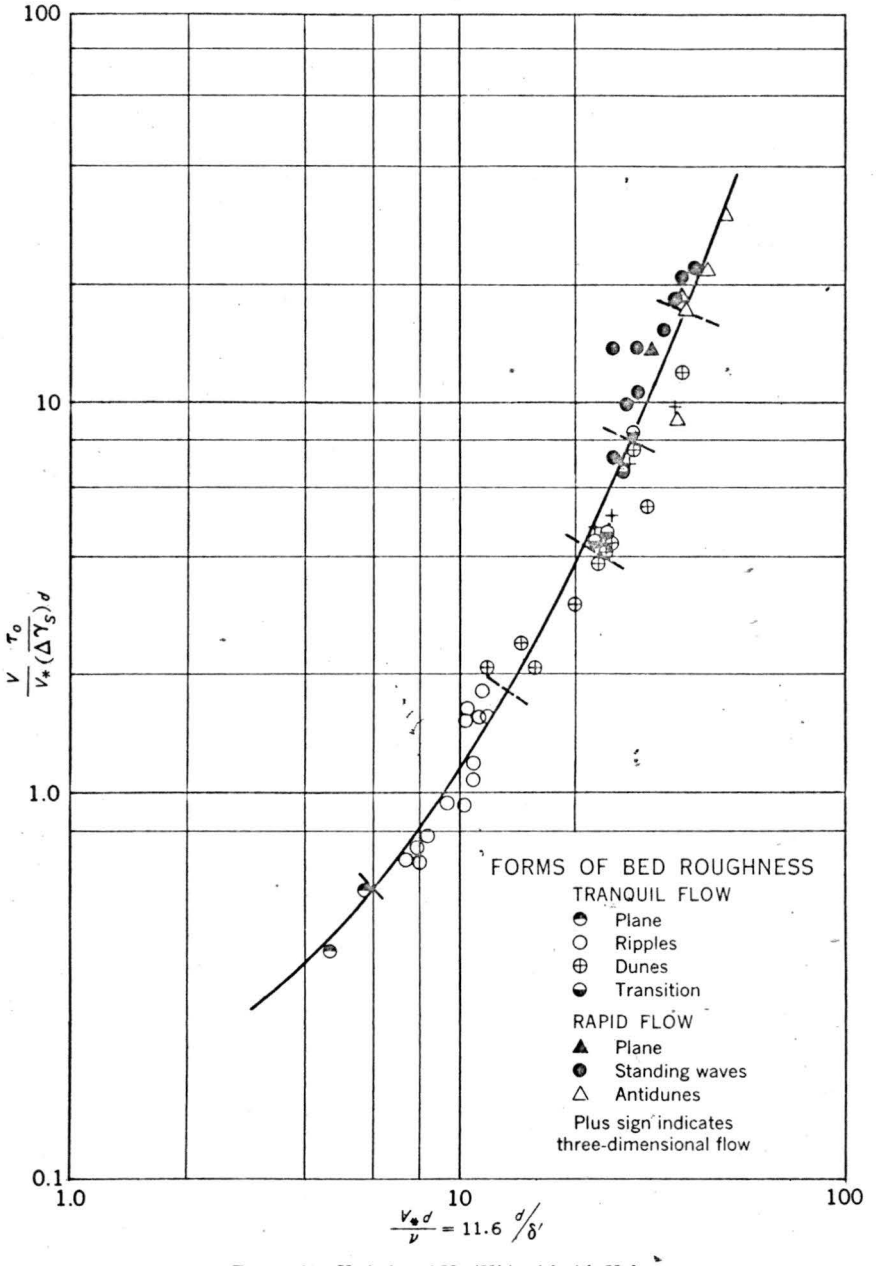

FIGURE 24.—Variation of $V\tau_0/V^*(\Delta\gamma_s)d$ with V_*d_*.

essentially straight, one line representing runs for $Fr>1$, the other line representing runs for $Fr<1$. These lines are shown in figure 25. Note that a constant equal to 5 was assumed. That is, figure 25 relates $(V_* d/)\nu+5$ to $V\ \tau_0/V_*(\Delta\gamma_s)d$. These two lines are combined into a single line in figure 26 by noting that the Froude number can

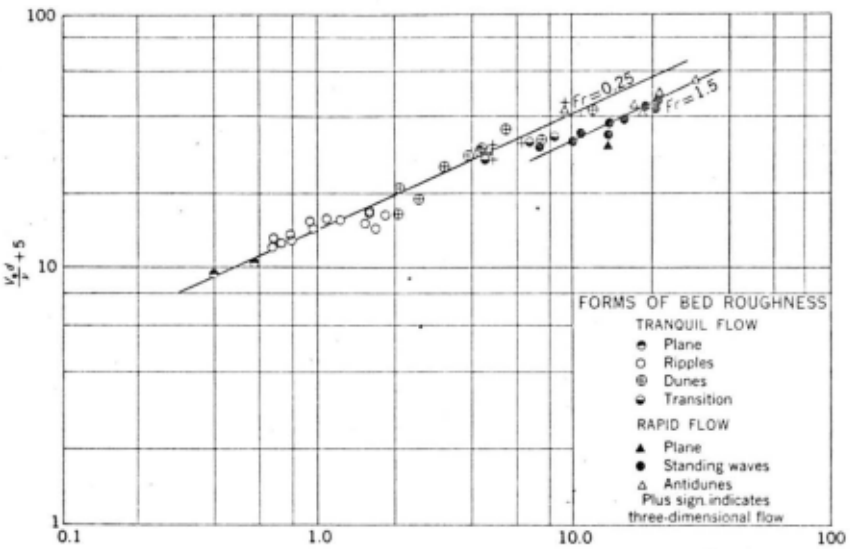

FIGURE 25.—Variation of $(V_* d/\nu)+5$ with $V\tau_0/V_*(\Delta\gamma_s)d$ and Fr.

be used as a third variable to evaluate a common intercept. The magnitude of this intercept (I) is.

$$I=12\left(\frac{V}{\sqrt{gD}}\right)^{-1/8}$$

and the equation of the resultant line becomes

$$\frac{V_* d}{\nu}+5=12.0\left[\frac{V}{V_*}\left(\frac{\tau_0}{\Delta\gamma_s d}\right)\right]^{0.445}\Big/\left(\frac{V}{\sqrt{gD}}\right)^{1/8} \tag{28}$$

The relation between $(V_* d/\nu)+5$ and $\dfrac{V}{V_*}\dfrac{\tau_0}{(\Delta\gamma_s)d}\Big/\left(\dfrac{V}{\sqrt{gD}}\right)^{1/8}$

is given in figure 26. The foregoing equation modified to conform with this figure becomes

$$\frac{V_* d}{\nu}+5=11.85\left(\frac{V}{V_*}\frac{\tau_0}{\Delta\gamma_s d}\right)^{0.465}\Big/\left(\frac{V}{\sqrt{gD}}\right)^{0.13} \tag{29}$$

Expressing this equation in the form of the Chezy equation

$$V=0.0049\left(\frac{V_* d}{\nu}+5\right)^{2.15}\left(\frac{V}{\sqrt{gD}}\right)^{0.28}\frac{\Delta\gamma_s d}{\gamma DS}\sqrt{gDS} \tag{30}$$

and

$$\frac{C}{\sqrt{g}}=0.0049\left(\frac{V_* d}{\nu}+5\right)^{2.15}(Fr)^{0.21}\frac{\Delta\gamma_s d}{\gamma DS} \tag{31}$$

The velocity term in the Froude number can be factored out and combined with the dependent variable for convenience.

All six forms of bed roughness are indicated in figure 26. Excluding some overlap of the runs having dune bedforms and the runs having transition bedforms, the forms of bed roughness plot in well-defined groups.

Equation 9 results from the dimensional analysis of the problem of channel roughness.

$$\phi_9\left[S,Re,Fr,\frac{d}{D},\frac{w}{V},C_D\right]=0 \tag{9}$$

Considering for the present that because d, w and C_D are interrelated, C_D and w may be of secondary importance and may be eliminated at least temporarily from equation 9. Then, the foregoing expression reduces to

$$Fr^2=\frac{V^2}{gD}=\phi\left[Re,S,\frac{d}{D}\right] \tag{32}$$

in which Fr has been squared arbitrarily. Taking the liberty of combining the remaining parameter as follows as a first approximation,

$$\frac{Fr^2}{Re}=\phi\left[\frac{Sd}{D}\right] \tag{33}$$

a plot can be made using $\frac{Fr^2}{Re}=\frac{V\mu}{\gamma D^2}=\phi\left[\frac{Sd}{D}\right]$ with $V_* D/\nu$ as the third variable. A family of parallel lines of constant $V_* D/\nu$ values can be established on log-log paper. This family of lines can be compressed into a narrower band by finding the equation relating the intercepts and values of $V_* D/\nu$ and replotting according to the indicated relationship. That is,

$$\frac{V\mu}{\gamma D^2}=\phi\left[\left(\frac{Sd}{D}\right)^{3/4}\left(\frac{\nu}{V_* D}\right)\right] \tag{34}$$

In doing so it is noted that Fr can be used as a third variable to yield a family of parallel lines, which can be reduced to a single line by

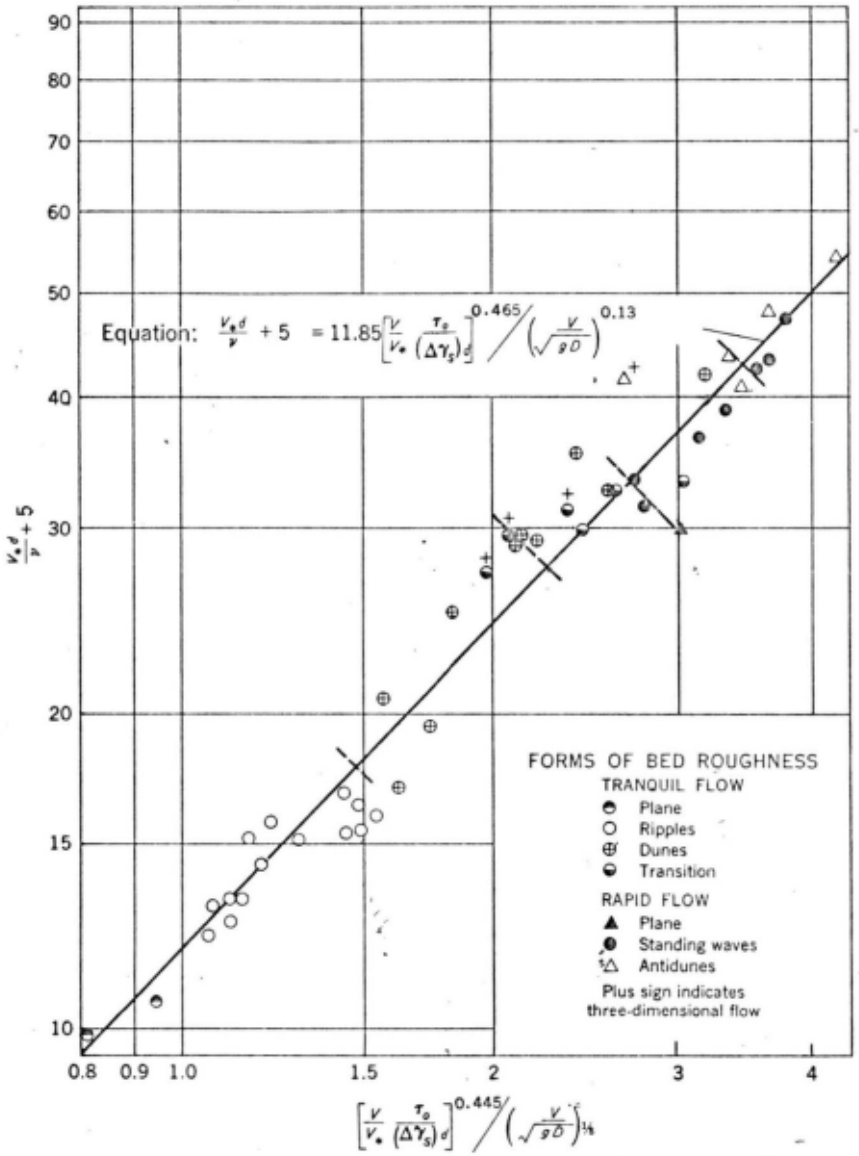

FIGURE 26.—Variation of $V_* d/\nu + 5$ with $[V\tau_0/V_*(\Delta\gamma_s)d]^{0.445}/(V/\sqrt{gD})^{1/4}$

again solving for the general intercept equation and substituting it in equation 34. Following this procedure the equation

$$\frac{V\mu}{\gamma D^2}\left(\frac{\sqrt{gD}}{V}\right)^{3/4} = K\left[\left(\frac{Sd}{D}\right)^{3/4}\frac{\nu}{V_* D}\right]^{2/3} \tag{35}$$

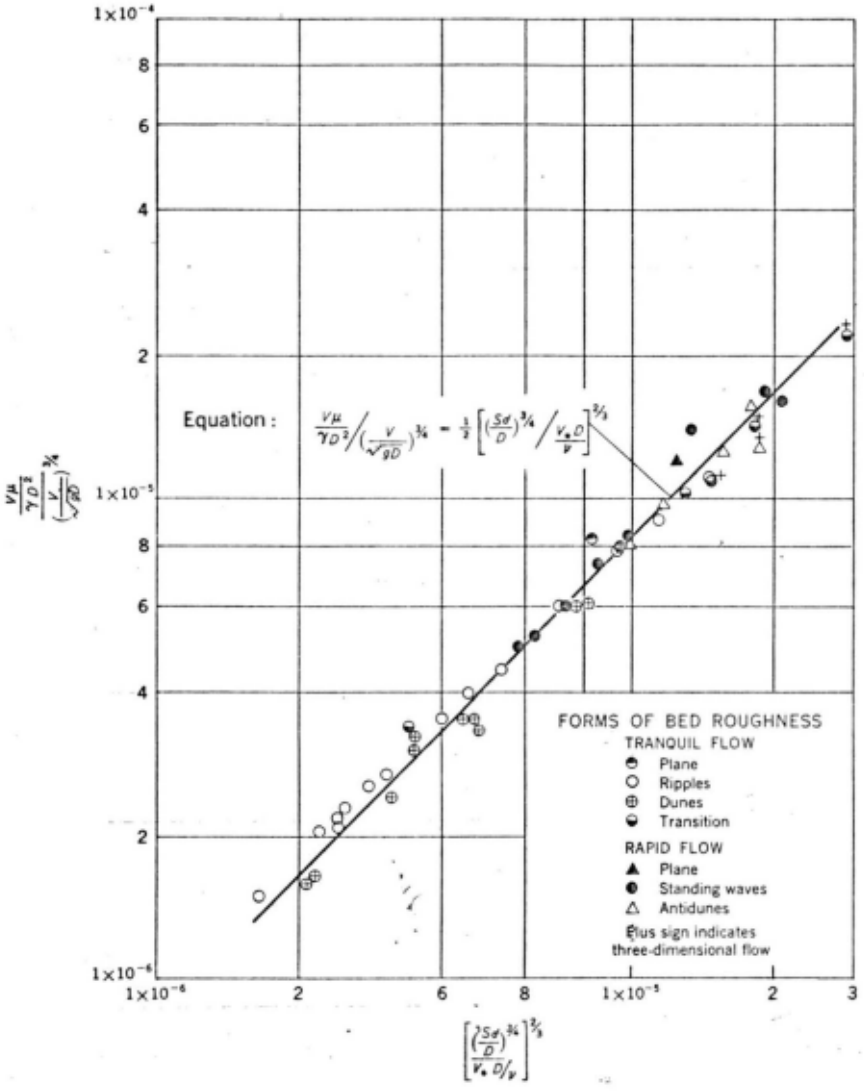

FIGURE 27.—Variation of $V\mu/\gamma D^2/(V/\sqrt{gD})^{3/4}$ with $[(Sd/D)^{3/4}/(V_* D/\nu)]^{2/3}$.

was obtained. This relation is presented in figure 27. Solving for V,

$$V=\frac{1}{2}S^{1/6}(C_D)^{2/3}\left(\frac{wd}{\nu}\right)^{4/3}\left(\frac{\gamma}{\Delta\gamma_s}\right)^{2/3}\sqrt{gDS} \tag{36}$$

and

$$\frac{C}{\sqrt{g}}=\frac{1}{2}S^{1/6}\,C_D{}^{2/3}\left(\frac{wd}{\nu}\right)^{4/3}\left(\frac{\gamma}{\Delta\gamma_s}\right)^{2/3} \tag{37}$$

where C_D, the drag coefficient of the particle, is equal to $\frac{\Delta\gamma_s d}{\rho w^2}$.

FORMS OF BED ROUGHNESS RELATED TO SIZE OF BED MATERIAL

As suggested in the introduction, a study of Liu's (1957) curve, which predicts when ripples form, led the writers to speculate on the possibility of discovering similar curves for other forms of bed roughness. As has been illustrated in the preceding figures, various parameters and (or) combinations of parameters apparently make it possible to define forms of bed roughness. In order to relate the foregoing concept to recent publications, the equation

$$\frac{V_*}{w}=\phi\left[\frac{V_* d}{\nu}\right] \tag{51}$$

was selected to test the concept. Therefore, figure 28 and table 2 were prepared using data from several sources, which are cited. In this figure it is clearly evident that, in general, dividing lines can be drawn to separate the forms of bed roughness. Furthermore, Liu's curve is extended more than one cycle to the left by means of the data of Kalinske and Hsia (1945), and it is extended more than one cycle to the right by the data of Lane and Carlson (1953). In this figure a temperature of 20°C was used to determine the fall velocity and kinematic viscosity where temperature was not available. The scatter among the points from Laursen (1958), Brooks (1957), Barton and Lin (1955) and the basic flume data is due in large part to the temperature variation. Lines of constant temperature can be drawn for these data at an angle of 45°. It is also noteworthy that for almost any transition line, a change in temperature for a given size of bed material can result in a change in the form of bed roughness.

The following are observations regarding figure 28 and table 2 that may have significance.

1. Kalinske and Hsia (1945) reported ripple formation, although they did not record the conditions under which movement began and the conditions under which ripples were initiated. The minimum value of d/δ' for their data is approximately at the same point where the Colebrook-White curve (Rouse, 1946) connects with the smooth boundary curve. To the left of this point the boundary is completely smooth, no influence of the overhead turbulence is felt at the boundary, and the laminar sublayer is a completely protective blanket. This fact makes it doubtful that ripples form under these conditions. In any event the authors have been unable to locate any data for smaller values of d/δ'. The instability of fine noncohesive materials may make it difficult to determine definitely when movement begins and ripples start to form.

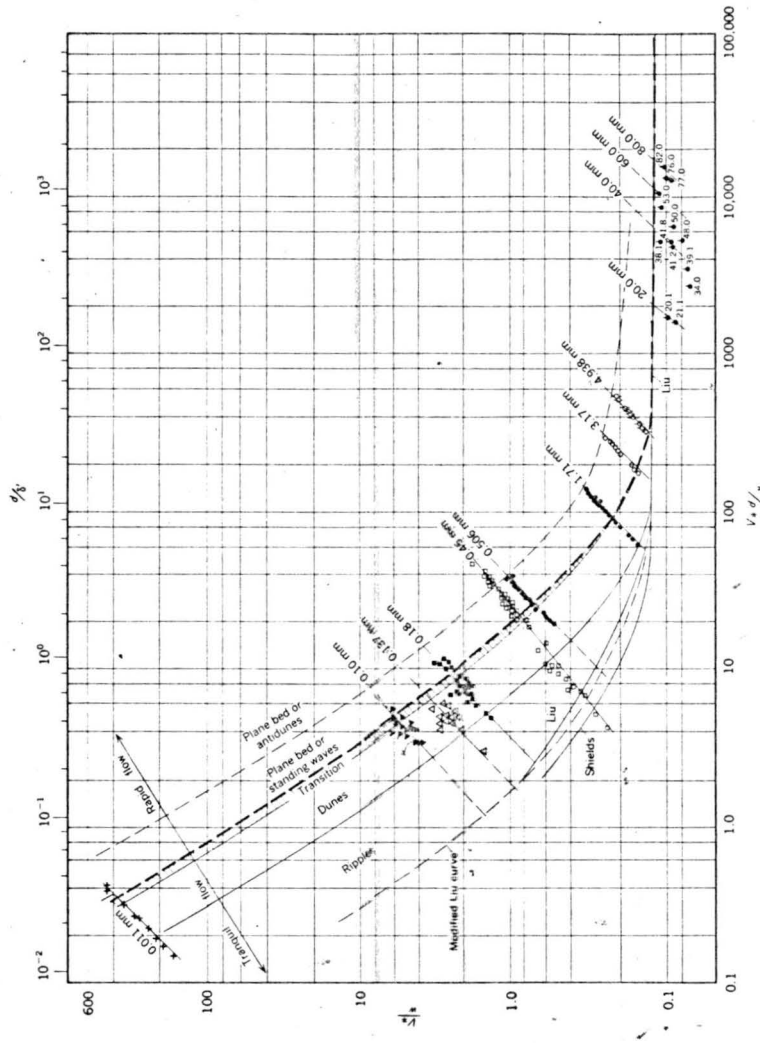

FIGURE 28.—Criteria for bed roughness in alluvial channels.

TABLE 2.—*Values for predicting bed form*

[Froude number, Fr; concentration of total load, C_T; slope for predicting bed forms, S]

Reference	Particle diameter (mm)	Point of transition from—											
		Plane bed to ripples			Ripples to dunes			Dunes to rapid-flow forms			Standing waves to antidunes		
		Fr (value)	C_T (ppm)	S (percent)	Fr (value)	C_T (ppm)	S (percent)	Fr (value)	C_T (ppm)	S (percent)	Fr (value)	C_T (ppm)	S (percent)
Kalinske-Hsia (1945)	0.011				0.30	17,000	0.025	0.50	60,000	0.10			
Laursen (1958)	.10							.90		.12			
Brooks (1955)	.137				.25	70	.070						
Barton-Lin (1955)	.18				.20	20	.044	.60	1,800	.12			
Simons-Richardson, table 1	.45	0.15	1	0.023	.30	90	.057	.60	3,000	30	1.20	4,000	.40
Gilbert (1914)	.506							.90	3,000	.50			
	1.71							1.0	2,000	.80			
	3.17							1.00	900	.90			
	4.94												
Lane-Carlson [1] (1953)	42.0												

[1] Complete stability of bed, no transition involved.

2. The curves describing the forms of bed roughness are rather clearly defined and are nearly parallel for $d/\delta' < 10$. In figure 28 it is apparent that Liu's curve is not parallel to the foregoing family of curves in this range, whereas the Shield's curve turns up at the left end more nearly in accordance with them. Based on the rather definite and systematic orientation of the regime curves and Shield's curve, it is possible that Liu's curve should be lowered in the vicinity of $d/\delta' = 1$. This results in a curve (fig. 28) that more nearly conforms to the curves defining the other regimes of flow. Such a minor adjustment might also be justified by a careful study of the effect of size distribution of the sediment.
3. For increasing values of d/δ' (the laminar sublayer becoming relatively thinner and thinner) the influence of viscosity becomes less and less for each type of bed formation. Ripples do not form beyond $d/\delta' \approx 10$ and dunes cease to exist beyond $d/\delta' \approx 40$. Apparently, the data are sufficiently complete to permit these approximate conclusions regarding both ripples and dunes. For bed formations of the rapid flow regime, however, the data are not complete enough for any conclusions to be drawn about whether the standing waves and antidunes ceases to exist beyond some large value of d/δ'.
4. Because of the large surface waves and irregularities in rapid flow regime, the Froude number no doubt plays a very important part. No attempt has been made as yet to relate the Froude number beyond that done in table 2 and as illustrated in figure 28.
5. Although the two variables V_*/w and $V_* d/\nu$, as shown by figure 28, are of primary importance, there is still need for a significant third variable that will correlate the data in a quantitative manner as now is done in a qualitative way by the terms, ripples, dunes, transition, plane bed, standing waves, and antidunes. The Froude number is significant, as shown in table 2, in defining ripples and dunes, but there is considerable question whether it will prove to be as significant for these forms of bed roughness as for the forms in the rapid flow regime. The drag coefficient C_D is essentially a constant for each size of bed material, and, hence, is not a logical third variable, except perhaps in establishing the points where the forms of roughness, such as ripples and dunes, may cease to exist. The remaining variables that might be significant are: the slope S, the size of bed material d relative to the depth of flow D, the concentration of total load C_T, the Chezy discharge coefficient $C/\sqrt{g}$, and the parameter used by Shields, $\tau_0/d\Delta\gamma_s$. Which of these would be most

significant depends, at least to some extent, upon the use of the plot.

6. Figure 28 shows that as d/δ' increases, the existence of two forms of the bed roughness are eliminated. When $d/\delta'>7$ and sediment is moving, the possibility of the first condition (movement without bed waves) is eliminated. When $d/\delta'>10$, ripples will no longer form, and when $d/\delta'>40$, dunes may not exist. For sediments with a specific gravity of 2.65, figure 28 shows that the changes in form of bed roughness are related approximately to the size of sediment, the limiting size for the existence of ripples, and dunes being approximately 2.5 mm, and 8 mm respectively. In the rapid flow regime beyond $d/\delta'=40$, several bed configurations are possible, such as a plane bed and a bed with symmetrical undulations of various sizes. The limiting conditions for the standing wave and antidune forms of bed roughness are not established. Although the factors that produce these limits are not known, they are no doubt related at least in part to the influence of viscosity as expressed by d/δ'. However, the limits may also be related to gravitational forces and the forces creating the sand waves, the drag coefficient, the size of the sand waves, the size of bed material, and the Froude number. Perhaps both ripples and dunes disappear when the grain roughness approaches the same order of magnitude as the size of the dunes and ripples.
7. Within the tranquil flow regime the form of bed roughness is unstable when $0.4<Fr<1.0$. Typical dunes cease to exist when $0.4<Fr<0.6$, depending on the characteristics of the bed material. The flow for which $(0.4 \text{ to } 0.6)<Fr<1.0$ is in the transition zone between dunes and rapid flow forms. The proximity of the transition zone to critical flow conditions $Fr=1$ probably accounts for the instability cited.
8. In the rapid flow regime following bed conditions occur:
   a. A plane bed forms with no visible sand waves of any kind and with a very smooth water surface. These flume studies showed that this condition is unstable and is difficult to reproduce, particularly as the length of flume is increased beyond 75 feet.
   b. Symmetrical standing waves of low amplitude form and gradually disappear. Unlike antidunes these water surface and bed waves have no tendency to migrate upstream or to break and shear off. The bed may be plane, have a diagonal dune pattern crisscrossed like shoestrings or have symmetrical undulations.

This change in flow regime from tranquil to rapid or vice versa may, if conditions are right, occur in a natural stream. That is, if the slope of the energy grade line is close to the critical slope, a change in stage results in a change in regime. When this occurs there is a break in the discharge rating curve. Because there is a hysteresis in the change, the stage where the break occurs varies depending on whether the stage is rising or falling and the rate of change of discharge with time.

The usefulness of the various equations for $C/\sqrt{g}$ developed in this report is severely limited by the range of data upon which they are based. As the influences of different bed materials, and a wider range of temperature conditions are determined, as a result of proposed future work, these expressions will undoubtedly need revisions, which will make them much more useful to the engineering profession because of the greater range of conditions considered.

In the series of runs upon which this report is based, the antidunes developed when $Fr>1.3$. This may or may not be the case for other bed materials. For values of $1.0<Fr<1.3$, water surface waves formed which rarely broke in true antidune fashion, and the sand waves underlying the water waves stayed in essentially the same position. There was a very little tendency for these waves to move in either the upstream or downstream direction. At values of $Fr>1.3\pm$, the water waves formed and broke in a rather systematic manner and the sand waves moved in the upstream direction. The sand waves associated with the water waves were approximately the same shape as the water waves, but on a reduced scale. The sand waves were about one-half the amplitude of the water waves. There was a tendency for the magnitude of the sand and water waves to increase in the downstream direction along the flume, particularly for those runs having $1.0<Fr<1.3\pm$. The magnitude of the sand and water waves increased with depth. Breaking of the water waves and the sand waves occurred when the elevation of the crest of a sand wave was approximately at the same elevation as the water surface in an adjacent trough. It is apparent that antidunes reforming and breaking result in the surging flow observed in some natural streams.

There is a definite break in the Froude number when the bed form is changing from dune beds to rapid-flow bed forms. Dunes do not occur with this bed material when the Froude number is greater than 0.6. Rapid flow starts when $Fr>1.0$. Flow with a Froude number between 0.6 and 1.0 had multiple forms of bed roughness.

Observations of the forms of bed roughness, of the way they develop, and of the way they move indicate that it may be possible to determine the magnitude and type of bed roughness (particularly dunes) by checking the manner in which the bed material is segregated within the beds of small and intermittent streams. This method cannot be

employed if the bed material is perfectly uniform and is not contaminated with any foreign matter, but this is a laboratory situation. Also, the appearance of the water surface seems to provide an excellent means of estimating the form of bed roughness.

LITERATURE CITED

Albertson, M. L., Simons, D. B., and Richardson, E. V., 1958, Discussion of mechanics of ripple formation: Am. Soc. Civil Engineers Jour., v. 84, no. HY1.

Ali, S. M., and Albertson, M. L., 1956, Some aspects of roughness in alluvial channels: Colorado State Univ., Dept. Civil Eng. pub., CER 56SMA16, Fort Collins.

Bagnold, R. A., 1956, The flow of cohesionless grains in fluids: Royal Soc. (London) Philos. Trans., v. 249, no. 964, p. 235–297.

Barton, J. R., and Lin, P. N., 1955, A study of sediment transport in alluvial channels: Colorado State Univ., Dept. of Civil Eng. pub., no. 55JRB2, Fort Collins, p. 43.

Blench, T., 1957, Regime behavior of canals and rivers: London, Butterworth Scientific Publications, p. 12–27.

Brooks, N. H., 1955, Mechanics of streams with movable beds of fine sand: Am. Soc. Civil Engineers Proc., v. 81, no. 668, p. 1–28.

——— 1957, Closure—Mechanics of streams with movable beds of fine sand: Am. Soc. Civil Engineers Jour., v. 83, no. HY2.

Colby, B. D., and Christensen, R. P., 1956, Visual accumulation tube for size analysis of sand: Am. Soc. Civil Engineers Jour., v. 82, no. HY3.

Durand, R., 1953, Basic relationships of the transportation of solids in pipes—Experimental research: Internat. Hydrol. Convention Proc., p. 89–103, Minneapolis, Minn.

Einstein, H. A., 1950, The bed-load function for sediment transportation in open channel flows: U.S. Dept. Agriculture Tech. Bull. 1026.

Einstein, H. A., and El-Sayed Ahamd, El-Samni, 1949, Hydrodynamic forces on a rough wall: Rev. Modern Physics, v. 21, no. 3, p. 520–523.

Einstein, H. A., and Barbarassa, N. L., 1951, River channel roughness: Am. Soc. Civil Engineers Proc., v. 77, no. 78, p. 12.

Gilbert, G. K., 1914, Transportation of debris by running water: U.S. Geol. Survey Prof. Paper 86.

Kalinske, A. A., and Hsia, C. H., 1945, Study of transportation of fine sediments by flowing water: Iowa State Univ., Studies in Eng. Bull. no. 29.

Lane, E. W., 1955, The importance of fluvial morphology in hydraulic engineering: Am. Soc. Civil Engineers Proc., v. 81, no. 745.

——— Carlson, E. J., 1953, Some factors affecting the stability of canals constructed in coarse granular materials: Internat. Hydrol. Convention Proc., p. 37–48.

Laursen, E. M., 1958, Total sediment load of streams: Am. Soc. Civil Engineers Jour., v. 84, no. HY1.

Leopold, L. B., and Maddock, T. Jr., 1953, The hydraulic geometry of stream channels and some physiographic implications: U.S. Geol. Survey Prof. Paper 252.

Liu, H. K., 1957, Mechanics of sediment-ripple formation: Am. Soc. Civil Engineers Jour., v. 83, no. HY2.

Shields, A., 1936, Anwendung der Ähnlichkeitsmechanik und der Turbulenzforschung auf die Geschiebbewegung: (Application of similarity principles and turbulence research to bed-load movement): p. 42 Mitt. (der Preussischen Versuchsanstalt für Wasserbau und Schiffbau, Heft 26, Berlin).

Rouse, H., 1946, Elementary mechanics of fluids: New York, John Wiley and Sons.

——— 1950, Editor, Engineering hydraulics: New York, John Wiley and Sons.

Simons, D. B., and Albertson, M. L., 1960, Uniform water conveyance channels in alluvial material: Am. Soc. Civil Engineers Jour., v. 86, no. HY5.

U.S. Inter-Agency Report No. 4, 1941, Method of analyzing sediment samples: U.S. Dept. Army, St. Paul, Minn.

Van Driest, E. R., 1946, One dimensional analysis and the presentation of data in fluid flow problems: Jour. Appl. Mechanics, v. 13.

U.S. GOVERNMENT PRINTING OFFICE : 1961 O—577663